Multi-lepton anomalies at the LHC and the impact on Higgs physics in e^+e^-

Bruce Mellado

For the Wits Institute for Collider Particle Physics and iThemba LABS

In collaboration with IHEP (Y. Fang et al.)

中国科学院高能物理研究所
Institute of High Energy Physics
Chinese Academy of Sciences

INSTITUTE FOR COLLIDER PARTICLE PHYSICS
UNIVERSITY OF THE WITWATERSRAND

NRF National Research Foundation

iThemba LABS Laboratory for Accelerator Based Sciences

CEPC2019, IHEP, Beijing, 19/11/19

Outline

- ❑The simplified model
- ❑Di-lepton or multilepton "problem"
  - ❑Opposite sign di-leptons
  - ❑Same sign leptons and three leptons
  - ❑Three b-jet final states
  - ❑Three lepton final states with a Z
- ❑Combination and the anatomy
- ❑Impact on Higgs physics

Views expressed here are of the authors only

arXiv:1506.00612
arXiv:1603.01208
arXiv:1606.01674
arXiv:1706.02477
arXiv:1706.06659
arXiv:1709.09419
arXiv:1711.07874
arXiv:1809.06344
arXiv:1901.05300
arXiv:1909.03969

The Simplified Model and 2HDM+S

The Hypothesis (from Run I)

arXiv:1506.00612
arXiv:1603.01208
arXiv:1606.01674

1. The starting point of the hypothesis is the existence of a boson, H, that contains Higgs-like interactions, with a mass in the range 250-280 GeV
2. In order to avoid large quartic couplings, incorporate a mediator scalar, S, that interacts with the SM and Dark Matter.
3. Dominance of H→Sh,SS decay over other decays

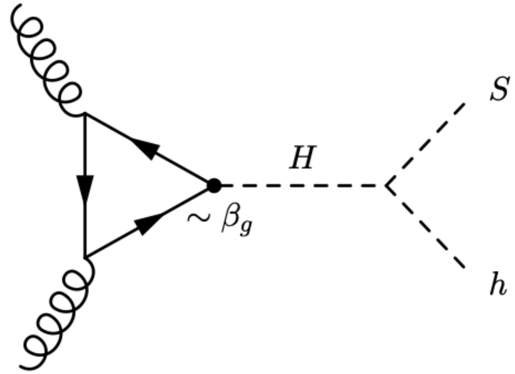

(a) Gluon fusion (ggF).

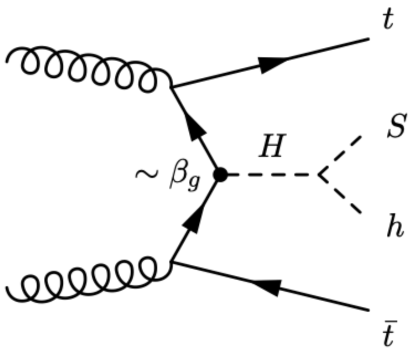

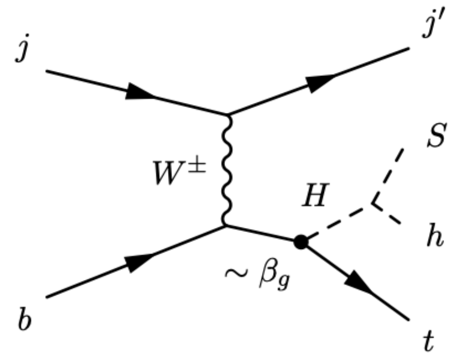

$$\mathcal{L}_{\rm int} \supset -\beta_g \frac{m_t}{v} t\bar{t}H + \beta_V \frac{m_V^2}{v} g_{\mu\nu} V^\mu V^\nu H$$

$$\mathcal{L}_{HhS} = -\frac{1}{2}\, v\Big[\lambda_{hhS} hhS + \lambda_{hSS} hSS + \lambda_{HHS} HHS + \lambda_{HSS} HSS + \lambda_{HhS} HhS\Big],$$

The 2HDM+S

arXiv:1606.01674

Introduce singlet real scalar, S.

2HDM potential, $\mathscr{V}(\Phi_1, \Phi_2)$

$$
\begin{aligned}
&= m_1^2 \Phi_1^\dagger \Phi_1 + m_2^2 \Phi_2^\dagger \Phi_2 - m_{12}^2 \left(\Phi_1^\dagger \Phi_2 + \text{h.c.}\right) \\
&+ \frac{1}{2}\lambda_1 \left(\Phi_1^\dagger \Phi_1\right)^2 + \frac{1}{2}\lambda_2 \left(\Phi_2^\dagger \Phi_2\right)^2 \\
&+ \lambda_3 \left(\Phi_1^\dagger \Phi_1\right)\left(\Phi_2^\dagger \Phi_2\right) + \lambda_4 \left|\Phi_1^\dagger \Phi_2\right|^2 \\
&+ \frac{1}{2}\lambda_5 \left[\left(\Phi_1^\dagger \Phi_2\right)^2 + \text{h.c.}\right] \\
&+ \left\{\left[\lambda_6 \left(\Phi_1^\dagger \Phi_1\right) + \lambda_7 \left(\Phi_2^\dagger \Phi_2\right)\right] \Phi_1^\dagger \Phi_2 + \text{h.c.}\right\}
\end{aligned}
$$

2HDM+S potential

$$
\begin{aligned}
&\mathscr{V}(\Phi_1, \Phi_2) + \frac{1}{2} m_{S_0}^2 S^2 + \frac{\lambda_{S_1}}{2} \Phi_1^\dagger \Phi_1 S^2 \\
&+ \frac{\lambda_{S_2}}{2} \Phi_2^\dagger \Phi_2 S^2 + \frac{\lambda_{S_3}}{4} (\Phi_1^\dagger \Phi_2 + \text{h.c}) S^2 \\
&+ \frac{\lambda_{S_4}}{4!} S^4 + \mu_1 \Phi_1^\dagger \Phi_1 S + \mu_2 \Phi_2^\dagger \Phi_2 S \\
&+ \mu_3 \left[\Phi_1^\dagger \Phi_2 + \text{h.c}\right] S + \mu_S S^3 .
\end{aligned}
$$

Out of considerations of simplicity, assume S to be Higgs-like, which is not too far fetched (see below)

The model leads to rich phenomenology. Of particular interest are multilepton signatures

S. No.	Scalars	Decay modes
D.1	h	$b\bar{b}$, $\tau^+\tau^-$, $\mu^+\mu^-$, $s\bar{s}$, $c\bar{c}$, gg, $\gamma\gamma$, $Z\gamma$, W^+W^-, ZZ
D.2	H	D.1, hh, SS, Sh
D.3	A	D.1, $t\bar{t}$, Zh, ZH, ZS, $W^{\pm}H^{\mp}$
D.4	$H^{\pm}$	$W^{\pm}h$, $W^{\pm}H$, $W^{\pm}S$
D.5	S	D.1, $\chi\chi$

Scalar	Production mode	Search channels
H	$gg \to H, Hjj$ (ggF and VBF)	Direct SM decays as in Table 1 $\to SS/Sh \to 4W \to 4\ell + E_T^{miss}$ $\to hh \to \gamma\gamma b\bar{b}$, $b\bar{b}\tau\tau$, $4b$, $\gamma\gamma WW$ etc. $\to Sh$ where $S \to \chi\chi \implies \gamma\gamma$, $b\bar{b}$, $4\ell + E_T^{miss}$
	$pp \to Z(W^{\pm})H$ $(H \to SS/Sh)$	$\to 6(5)l + E_T^{miss}$ $\to 4(3)l + 2j + E_T^{miss}$ $\to 2(1)l + 4j + E_T^{miss}$
	$pp \to t\bar{t}H, (t+\bar{t})H$ $(H \to SS/Sh)$	$\to 2W + 2Z + E_T^{miss}$ and b-jets $\to 6W \to 3$ same sign leptons + jets and E_T^{miss}
$H^{\pm}$	$pp \to tH^{\pm}$ $(H^{\pm} \to W^{\pm}H)$	$\to 6W \to 3$ same sign leptons + jets and E_T^{miss}
	$pp \to tbH^{\pm}$ $(H^{\pm} \to W^{\pm}H)$	Same as above with extra b-jet
	$pp \to H^{\pm}H^{\mp}$ $(H^{\pm} \to HW^{\pm})$	$\to 6W \to 3$ same sign leptons + jets and E_T^{miss}
	$pp \to H^{\pm}W^{\pm}$ $(H^{\pm} \to HW^{\pm})$	$\to 6W \to 3$ same sign leptons + jets and E_T^{miss}
A	$gg \to A$ (ggF)	$\to t\bar{t}$ $\to \gamma\gamma$
	$gg \to A \to ZH$ $(H \to SS/Sh)$	Same as $pp \to ZH$ above, but with resonance structure over final state objects
	$gg \to A \to W^{\pm}H^{\mp}(H^{\mp} \to W^{\mp}H)$	$6W$ signature with resonance structure over final state objects

Eur.Phys.J. C76 (2016) no.10, 580

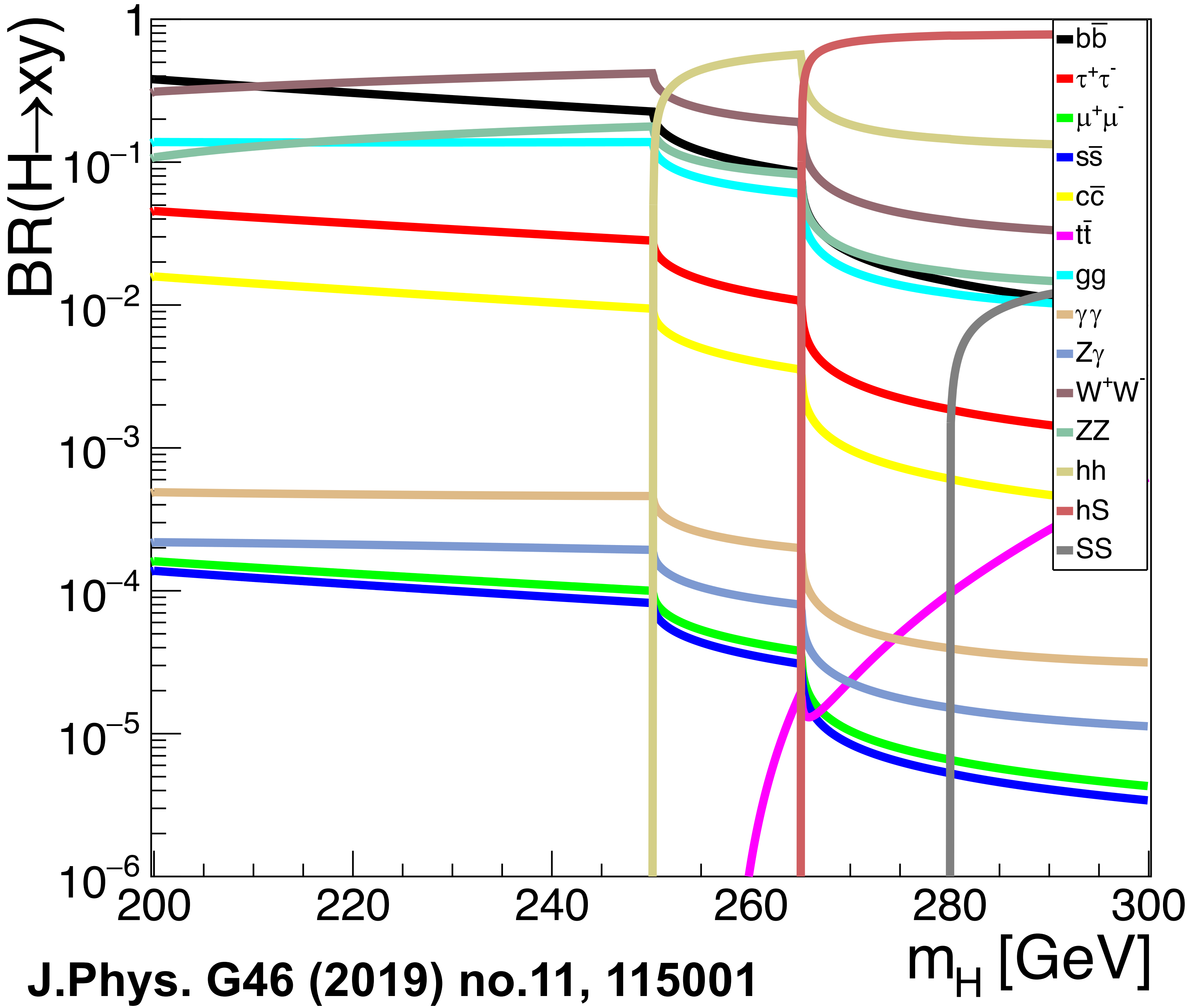

J.Phys. G46 (2019) no.11, 115001

Multi-lepton final states

$$pp \to H \to Sh$$
$$\to \ell^+ \ell^- + X$$

Expect di-leptons (m_{ll}<100 GeV) with jets and b-jets with rates comparable to that of the SM Higgs boson

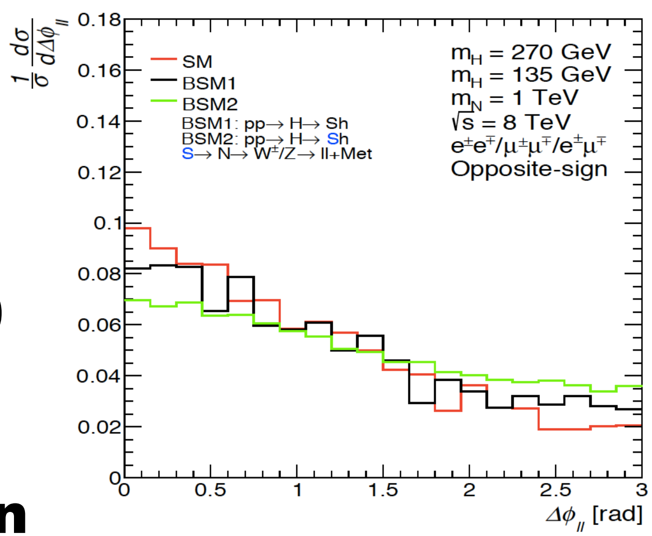

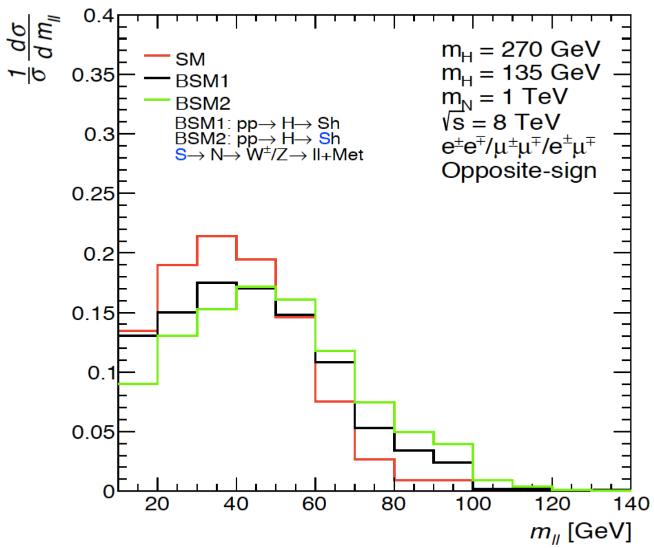

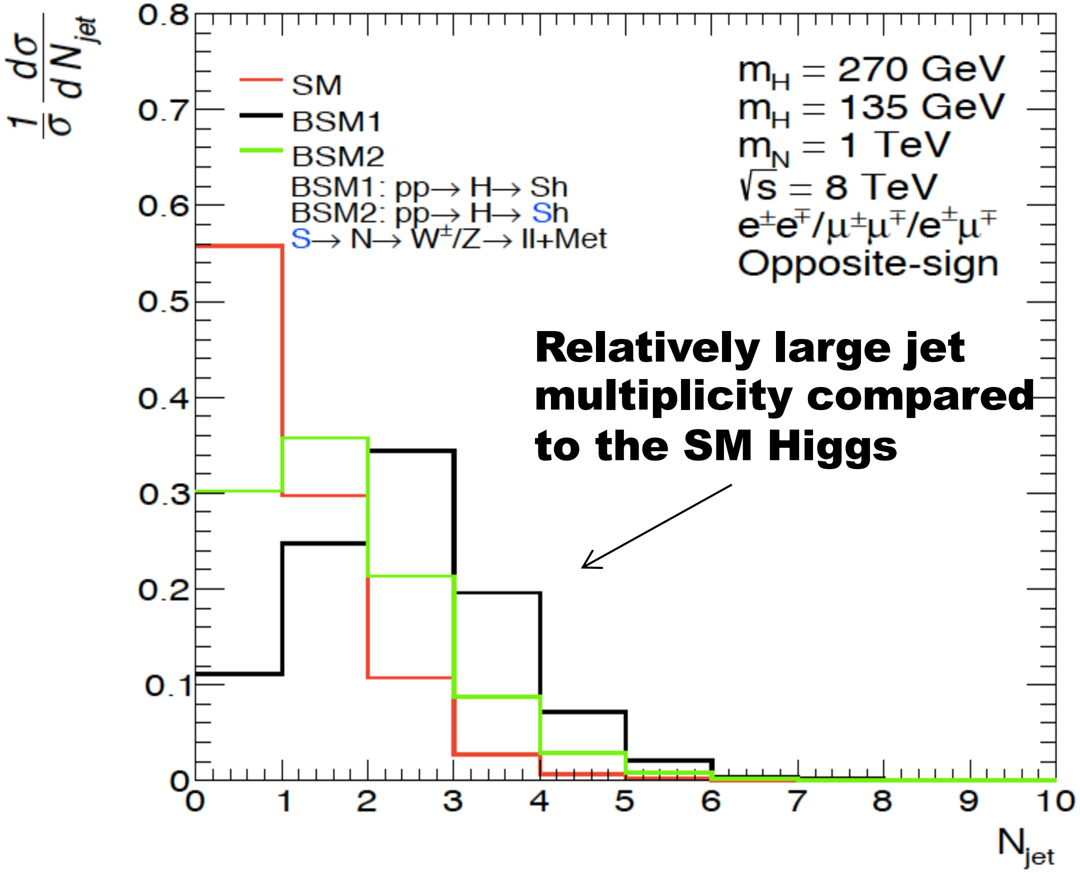

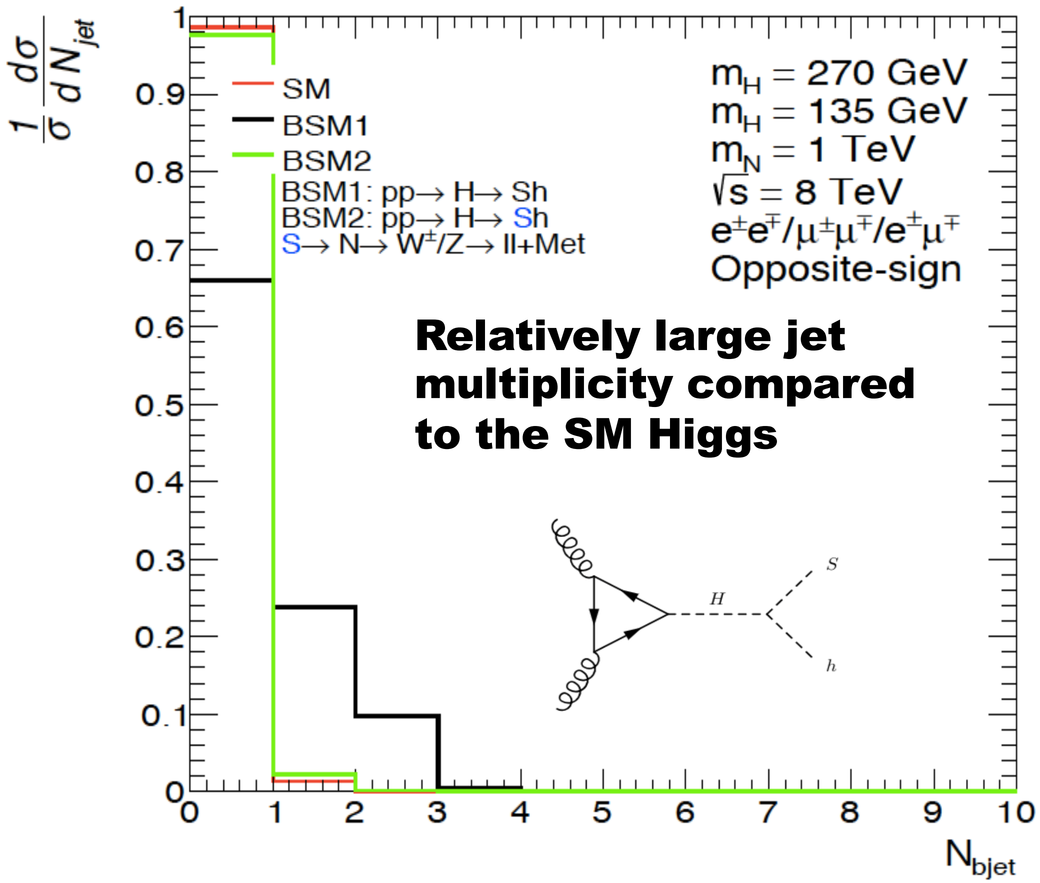

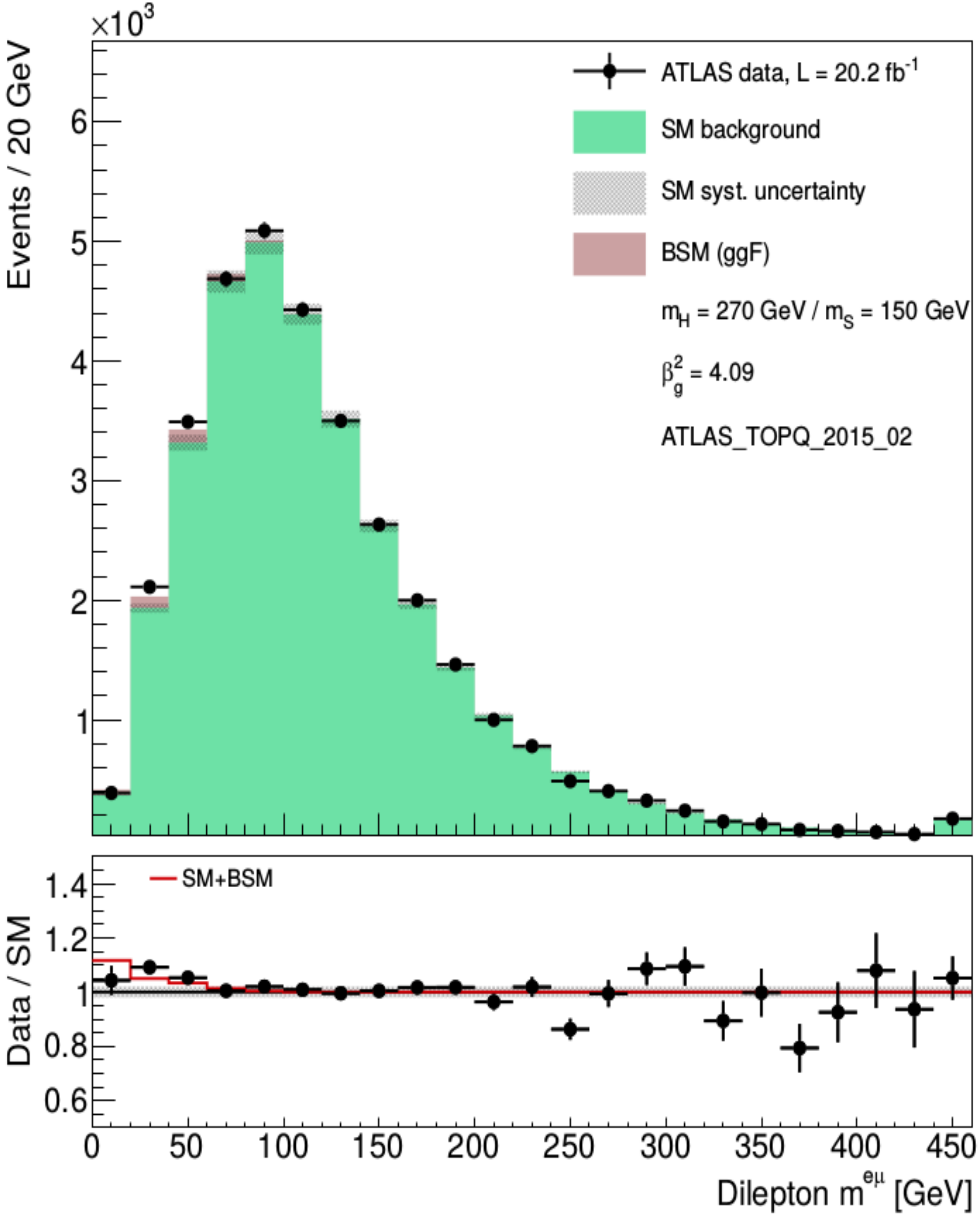

Simple selection:

- One DFOS lepton pair
- At least 1 *b*-tagged jet

We fix the normalisation of the SM by scaling it to the data in the region m_{ll} > 110 GeV

- Scale factor: 0.984
- A normalisation systematic of 2% is applied
- The fit is done to the region below 110 GeV

Fit results:

- $\beta_g^2 = 4.09 \pm 1.37$

Discrepancy in ATLAS is localized at small values of m_{ll}

CMS PAS TOP-17-014

Event selection with exactly two leptons (e,μ), m_{ll}>20 GeV and at least 2b-jets

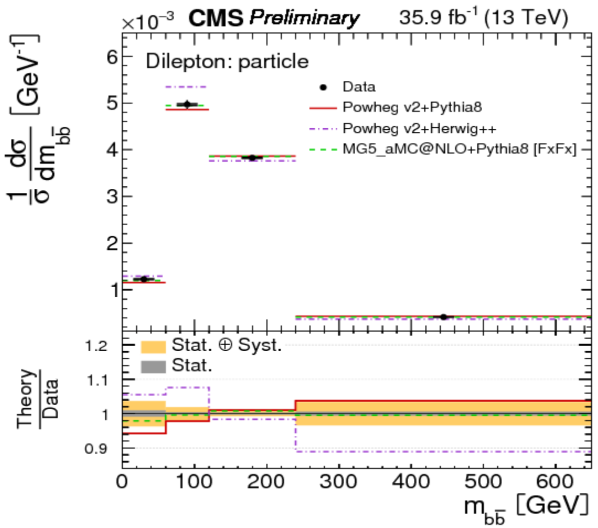

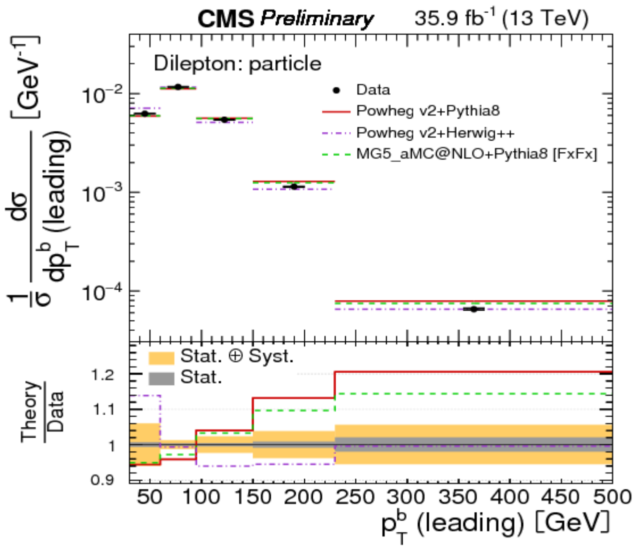

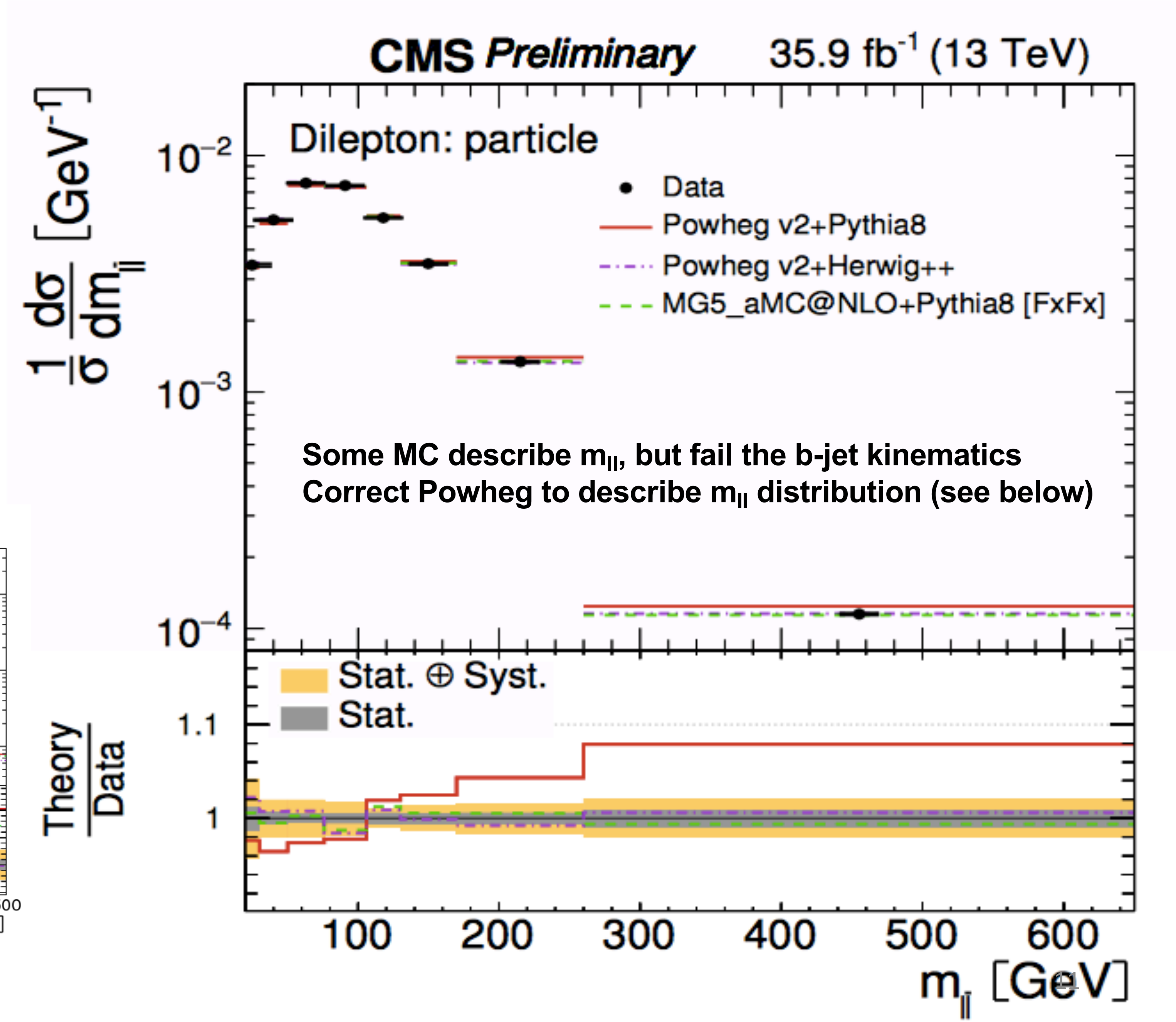

arXiv:1805.07399

CMS-TOP-17-018; CERN-EP-2018-074

- Poor modeling of POWHEG + Pythia8 distribution is improved through reweighting
- We fix the normalisation of the SM by scaling it to the data in the region m_{ll} > 110 GeV
  - A normalisation systematic of 3% is applied to all but DY
  - DY systematic = 6.8%. 3% systematic on m_{ll} shape in top
  - The fit is done to the region below 110 GeV
- Fit results:
  - $\beta_g^2 = 2.79 \pm 0.52$
  - Fit is extremely well constrained

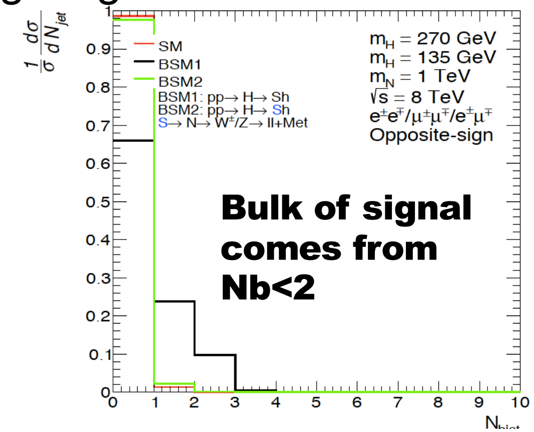

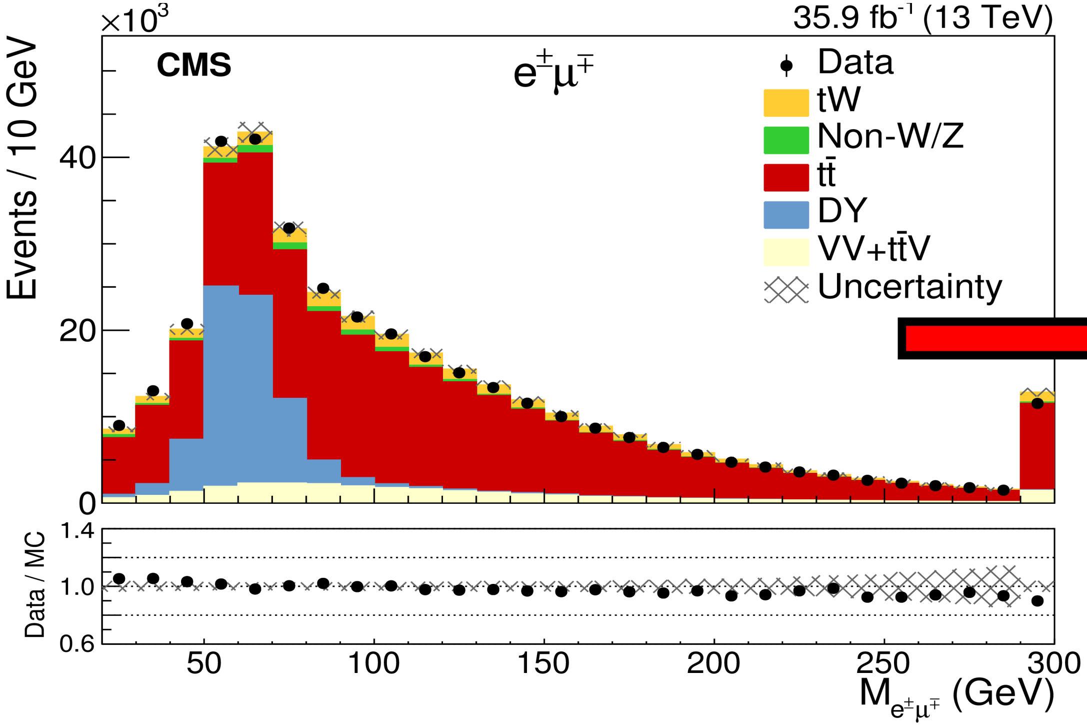

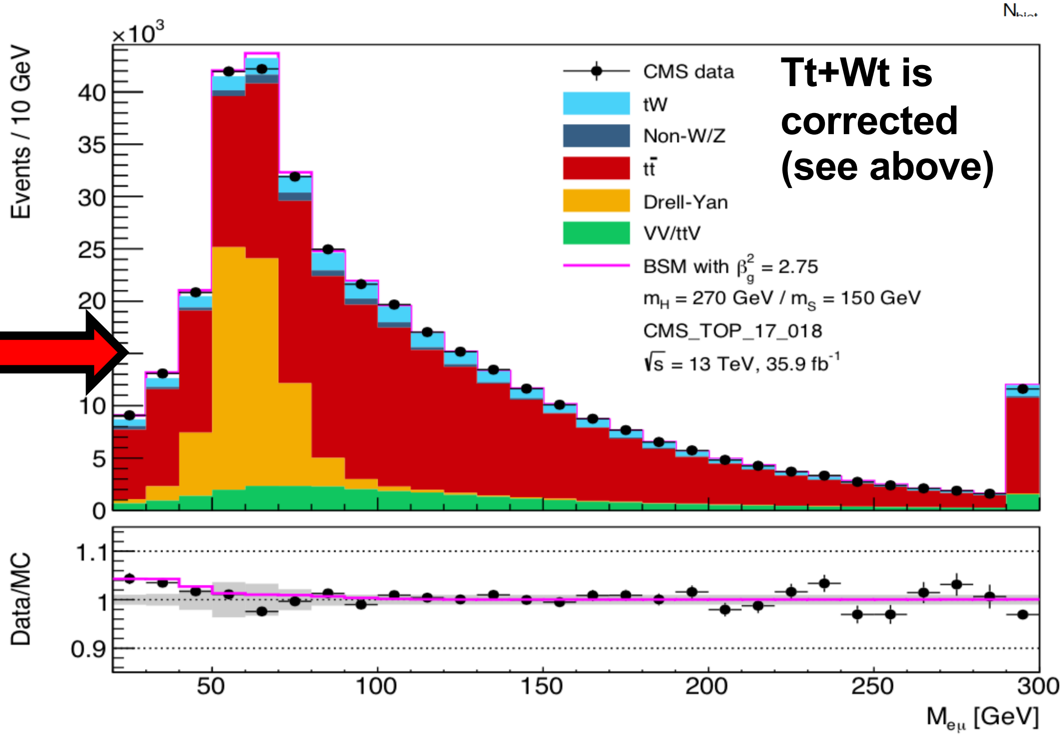

Used conservative assumption that ll+2b-jet final state is perfectly described by the SM. The discrepancy comes from events with N_b<2. Impacts h→WW→ll

Top associated Higgs production
(Multi-lepton final state)s

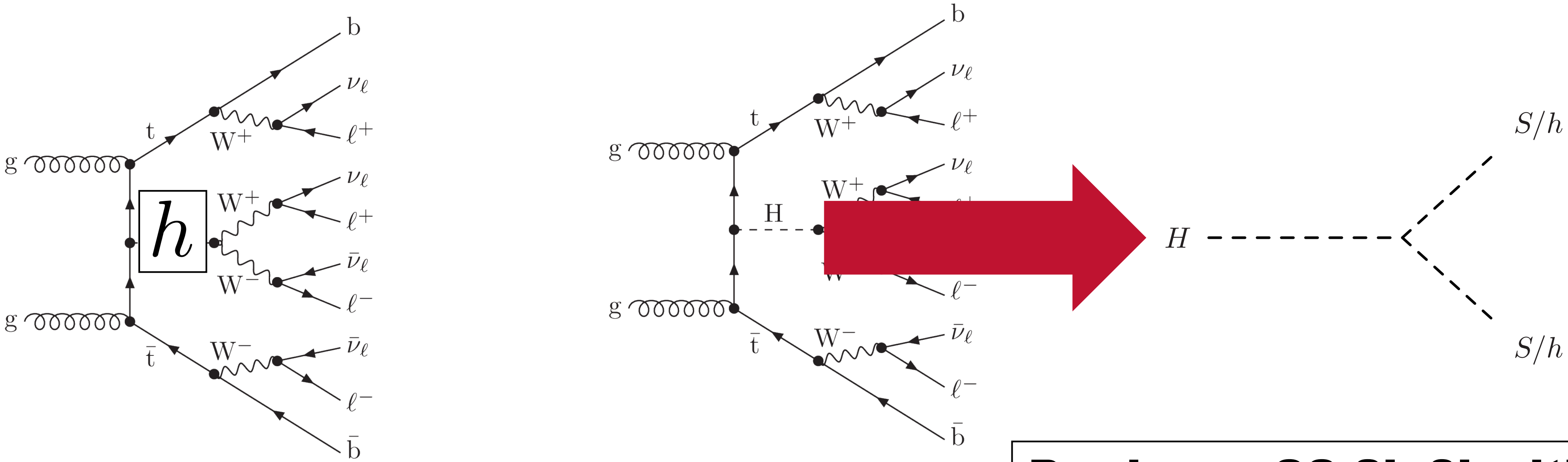

Reduced cross-section of ttH+tH is compensated by di-boson, (SS, Sh) decay and large Br(S→WW). Production of same sign leptons, three leptons is enhanced. Enhanced tH cross-section

Produces SS 2l, 3l with b-jets, including 3 b-jets

Explains anomalously large ttW+tth cross-sections seen by ATLAS and CMS

3l with Z→ll (ZW cross-section)

CMS PAS SMP-18-002

Errors in the plot are dominated by the 15% uncertainty on normalization to account NLO/NNLO differences. The uncertainty of the shape is much smaller of order of few %

Source	Combined	eee	$ee\mu$	$\mu\mu e$	$\mu\mu\mu$
Electron efficiency	1.9	5.9	3.9	1.9	0
Electron scale	0.3	0.9	0.2	0.6	0
Muon efficiency	1.9	0	0.8	1.8	2.6
Muon scale	0.5	0	0.7	0.3	0.9
Trigger efficiency	1.9	2.0	1.9	1.9	1.8
Jet energy scale	0.9	1.6	1.0	1.7	0.8
B-tagging (id.)	2.6	2.7	2.6	2.6	2.4
B-tagging (mis-id.)	0.9	1.0	0.9	1.0	0.7
Pileup	0.8	0.9	0.3	1.3	1.4
ZZ	0.6	0.7	0.4	0.8	0.5
Nonprompt norm.	1.2	2.0	1.2	1.5	1.0
Nonprompt (EWK subs.)	1.0	1.5	1.0	1.3	0.8
VVV norm.	0.5	0.6	0.6	0.6	0.5
VH norm.	0.2	0.2	0.3	0.2	0.2
$t\bar{t}$ V norm.	0.5	0.5	0.5	0.5	0.5
tZq norm.	0.1	0.1	0.1	0.1	0.1
X+γ norm.	0.3	0.8	0	0.7	0
Total systematic	4.7	7.8	5.8	5.7	4.6
Luminosity	2.8	2.9	2.8	2.9	2.8
Statistical	2.1	6.0	4.8	4.1	3.1
Total experimental	6.0	10.8	8.0	7.5	6.3
Theoretical	0.9	0.9	0.9	0.9	0.9

Systematics that will directly affect the shape (ZZ through X+γ norm.)

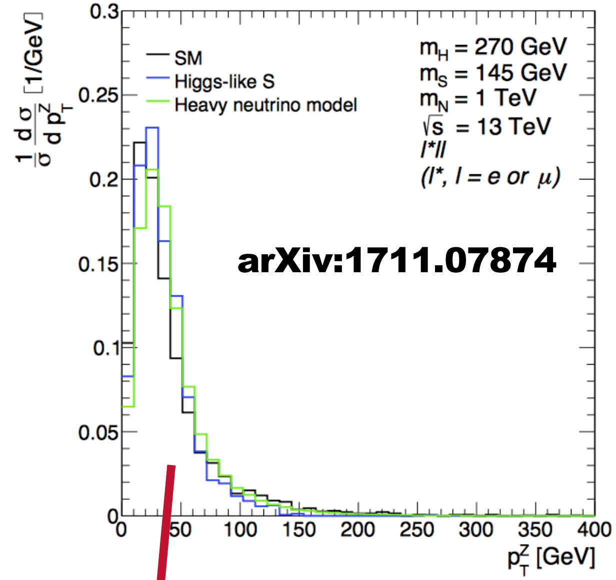

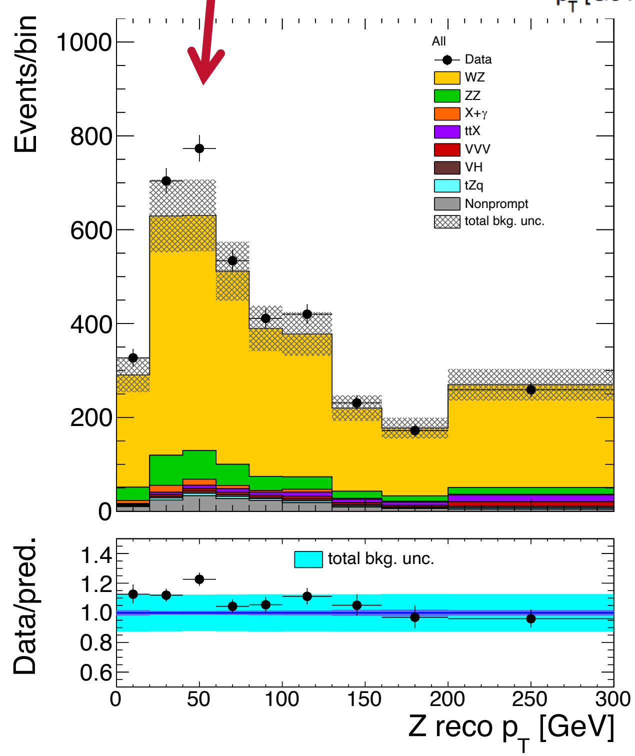

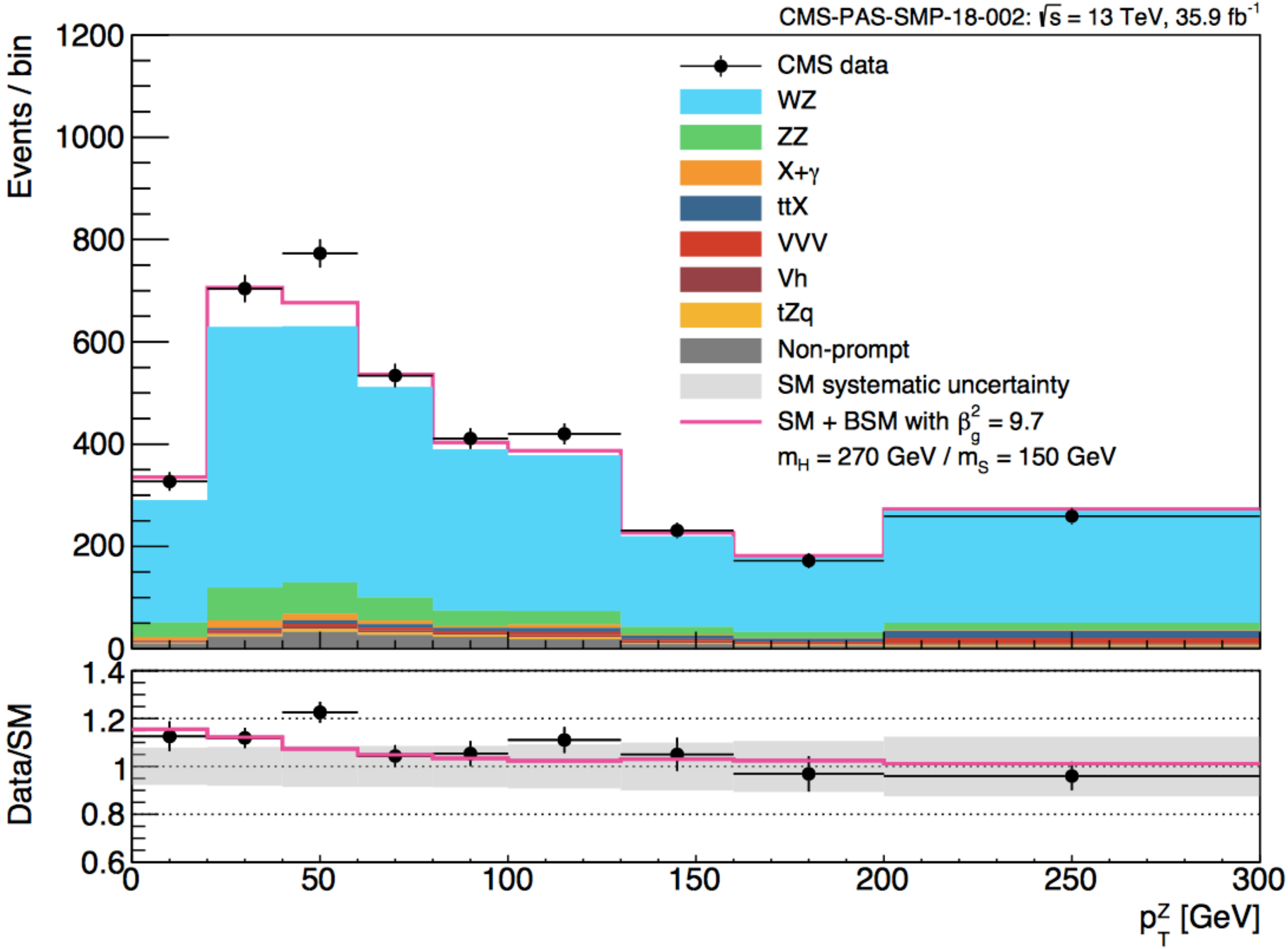

CMS-PAS-SMP-18-002: √s = 13 TeV, 35.9 fb-1
Events / bin
CMS data
WZ
ZZ
X+γ
ttX
VVV
Vh
tZq
Non-prompt
SM systematic uncertainty
SM + BSM with β2g = 9.7
mH = 270 GeV / mS = 150 GeV
Data/SM
pTZ [GeV]

BSM inputs to the fit

- **The following <u>assumptions</u> are made:**
  a. **The masses of *H* and *S* are fixed to m_H = 270 GeV and m_S = 150 GeV**
  b. **The only significant production mechanisms of *H* come from the *t*-*t*-*H* Yukawa coupling:**
     - **Gluon fusion**
     - **Top associated production**
  c. **The Yukawa coupling is scaled away from the SM Higgs-like value by the free parameter β_g**
  d. **The BR of $H \rightarrow Sh$ is fixed to 100%**
  e. **The BRs of *S* are Higgs-like**
- **Therefore, the only free parameter in the fits is β_g^2**

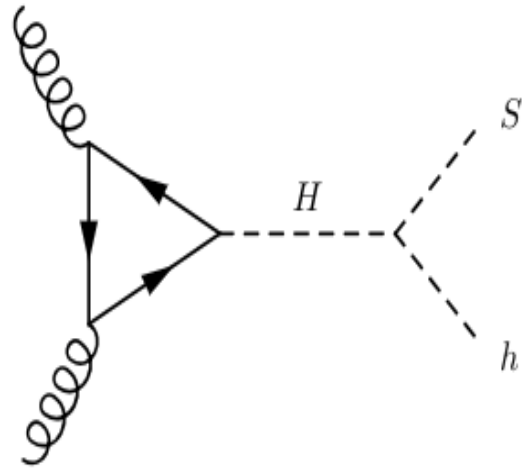

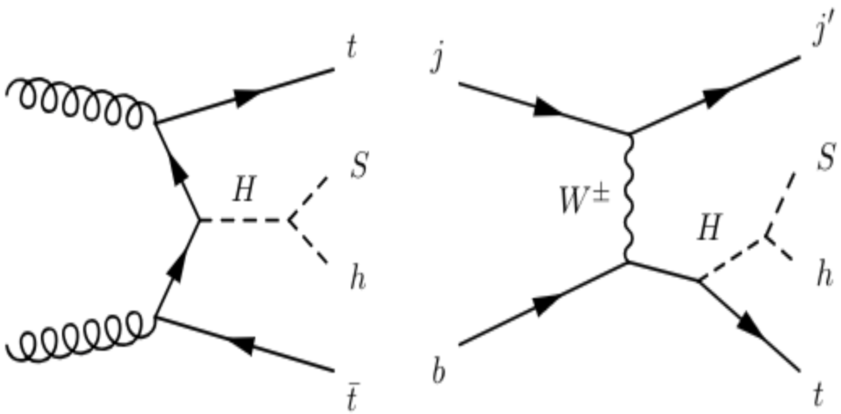

Selection	Best-fit β_g^2	Significance
ATLAS Run 1 SS leptons + b-jets	6.51 ± 2.99	2.37σ
ATLAS Run 1 DFOS di-lepton + b-jets	4.09 ± 1.37	2.99σ
ATLAS Run 2 SS leptons + b-jets	2.22 ± 1.19	2.01σ
CMS Run 2 SS leptons + b-jets	1.41 ± 0.80	1.75σ
CMS Run 2 DFOS di-lepton	2.79 ± 0.52	5.45σ
ATLAS Run 2 DFOS di-lepton + b-jets	5.42 ± 1.28	4.06σ
CMS Run 2 tri-lepton + $E_{\mathrm{T}}^{\mathrm{miss}}$	9.70 ± 3.88	2.36σ
ATLAS Run 2 tri-lepton + $E_{\mathrm{T}}^{\mathrm{miss}}$	9.05 ± 3.35	2.52σ
Combination	2.92 ± 0.35	8.04σ

The simplidied model seems to describe the discrepancies in different corners of the phase-space with large differences in cross-sections, eg, OS and SS di-leptons

Combination of fit results

- Simultaneous fit for all measurements:
- To the right: (-2 log) profile likelihood ratio for each individual result and the combination of them all
- The significance for each fit is calculated as

$$\sqrt{-2\log\lambda(0)}$$

- Best-fit: $\beta_g^2 = 2.92 \pm 0.35$
- Corresponds to 8.04σ

JHEP 1910 (2019) 157

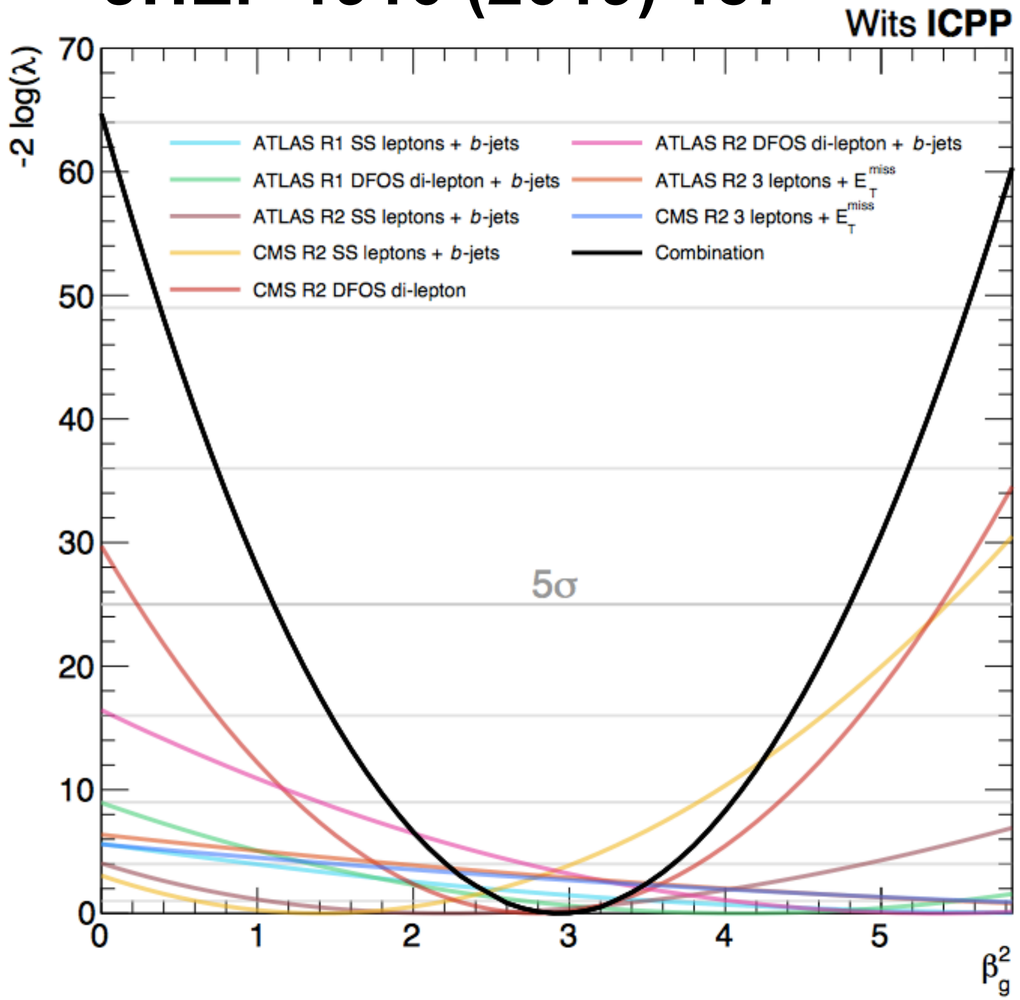

Interpretation: Measure of the inability of current MC tools to describe multiple-lepton data and how a simplified model with H→Sh is able to capture the effect with one parameter

Excesses in di-leptons with full-jet veto not included above

Run 1, J.Phys. G45 (2018) no.11, 115003

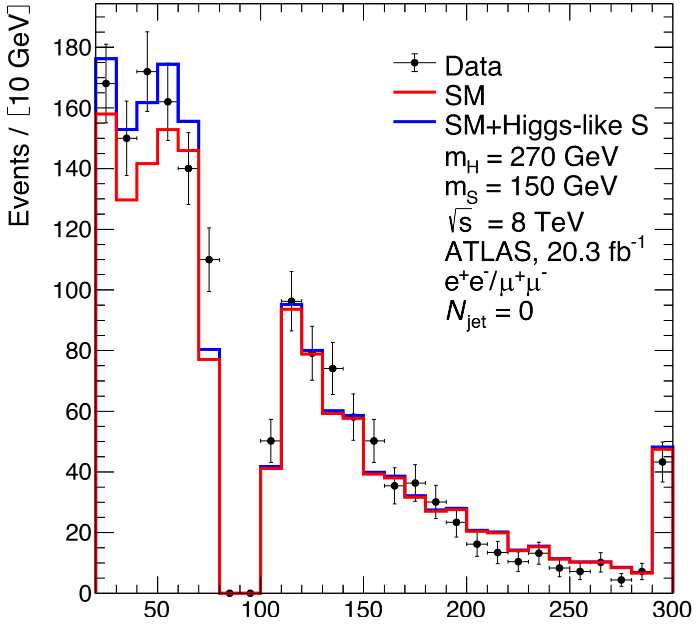

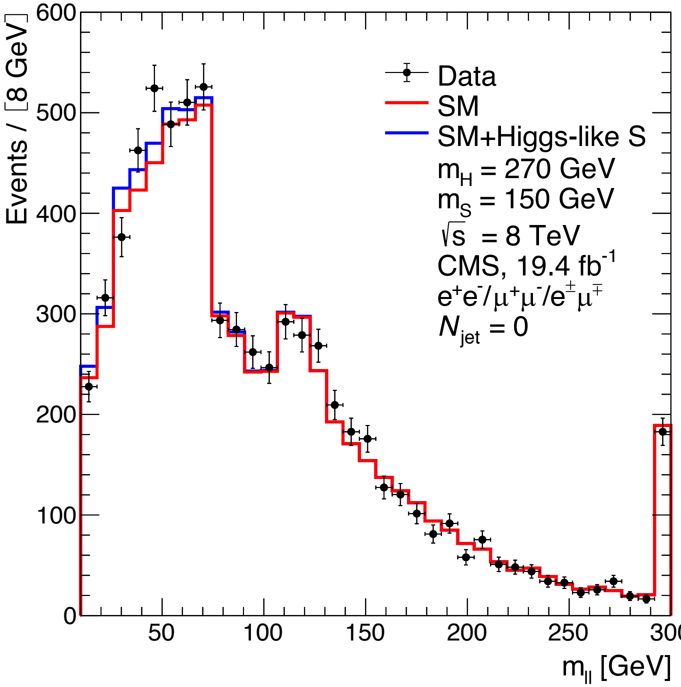

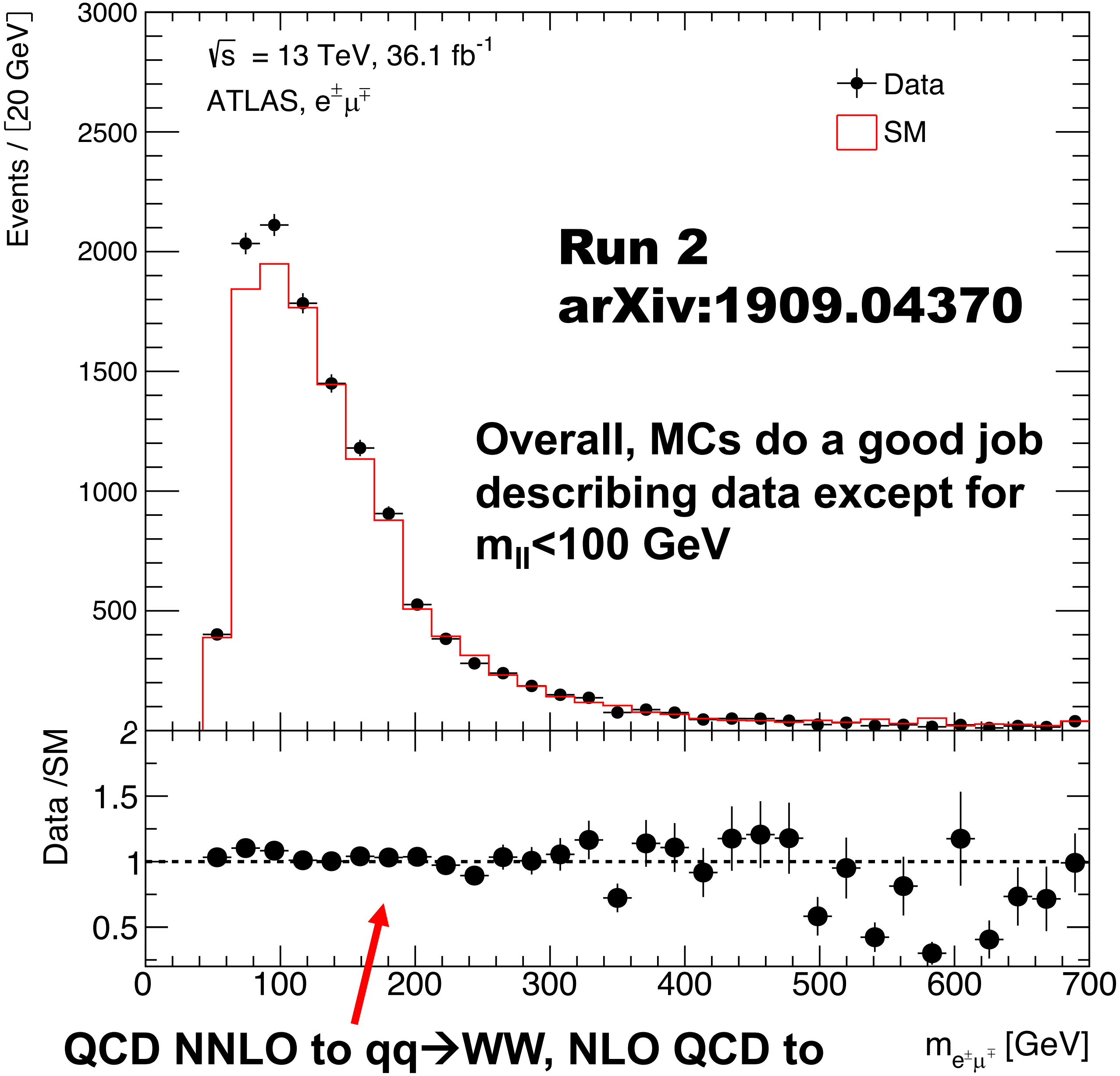

Run 2
arXiv:1909.04370

Overall, MCs do a good job describing data except for m_{ll}<100 GeV

QCD NNLO to qq→WW, NLO QCD to gg→WW and NLO EW corrections applied

arXiv:1910.08819

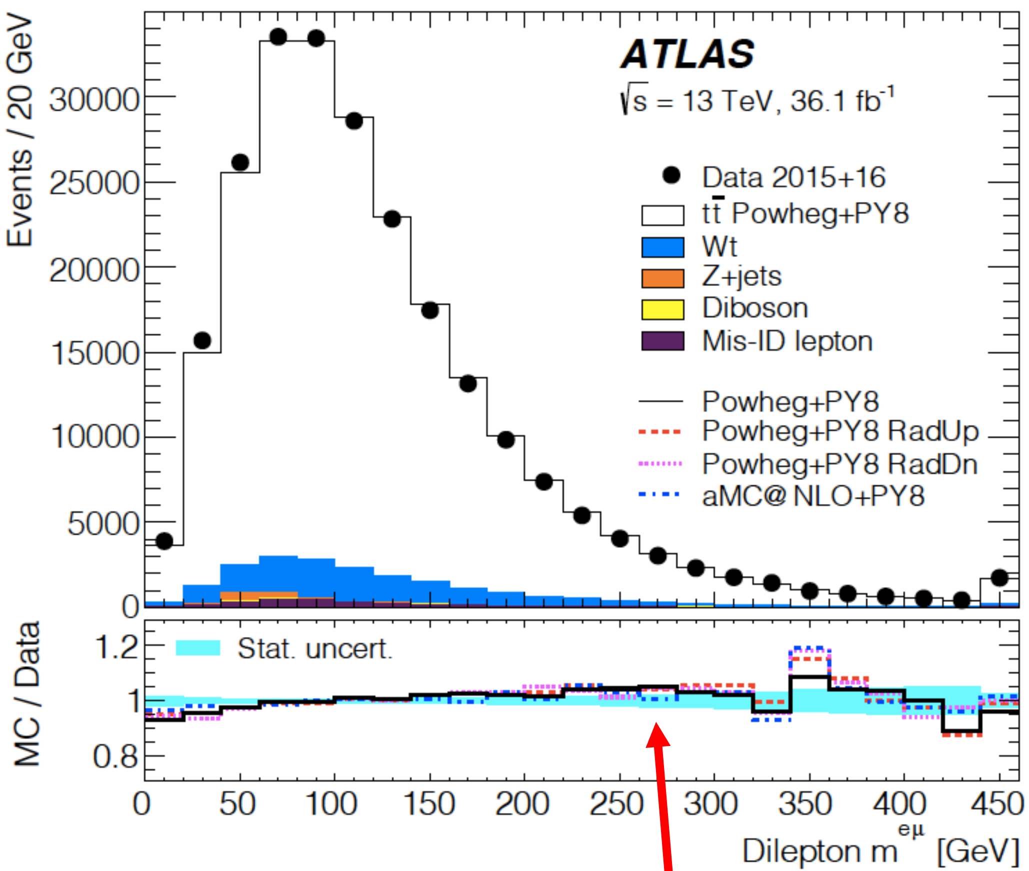

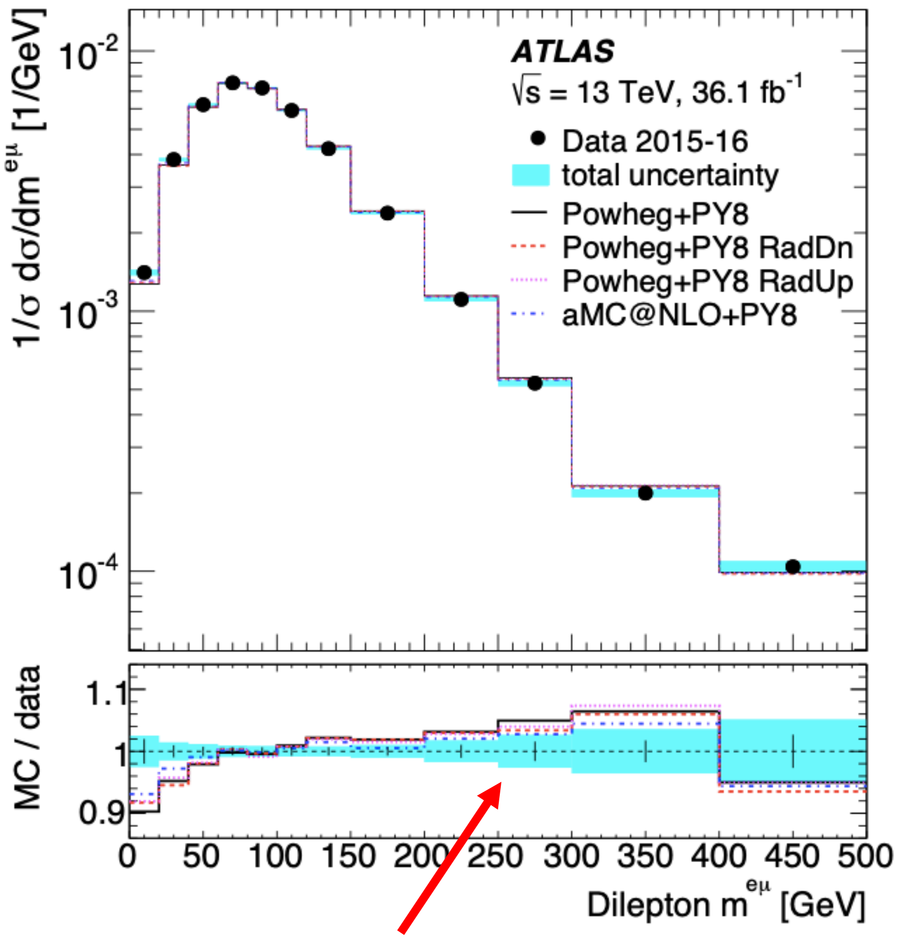

Residual discrepancies at high m_{ll} will be fixed with missing NNLO QCD and NLO EW corrections

Excess at low mll remains prevalent, indicating that effects seen in Run 1 were not statistical fluctuations. Preliminary NNLO QCD corrections do not fix the issue (see Mitov et al.)

Anatomy of the multi-lepton anomalies

JHEP 1910 (2019) 157

Final state	Characteristic	Dominant SM process
l^+l^- + jets, b-jets	m_{ll}<100 GeV, dominated by 0b-jet and 1b-jet	tt+Wt
l^+l^- + full-jet veto	m_{ll}<100 GeV	WW
$l^{\pm}l^{\pm}$ + b-jets	Excess with $N_{\pm}$>2, moderate H_T	ttV
$l^{\pm}l^{\pm}l$ + b-jets	Moderate H_T	ttV
$Z(\rightarrow l^+l^-)+l$	p_{TZ}<100 GeV	ZW

Anomalies cannot be explained by mismodelling of a particular process, e.g. ttbar production

Impact on Higgs Physics

The presence of a BSM signal of the type H→Sh would lead to:

- ❑ **Elevated cross-sections**
  - **Currently the measured h signal strength is**

$$\mu = 1.133 \pm 0.054(\text{exp.})$$

- ❑ **The presence of extra leptons in association with h. Affects the Wh measurement**
- ❑ **Distortion of Higgs p_T and rapidity (under study)**

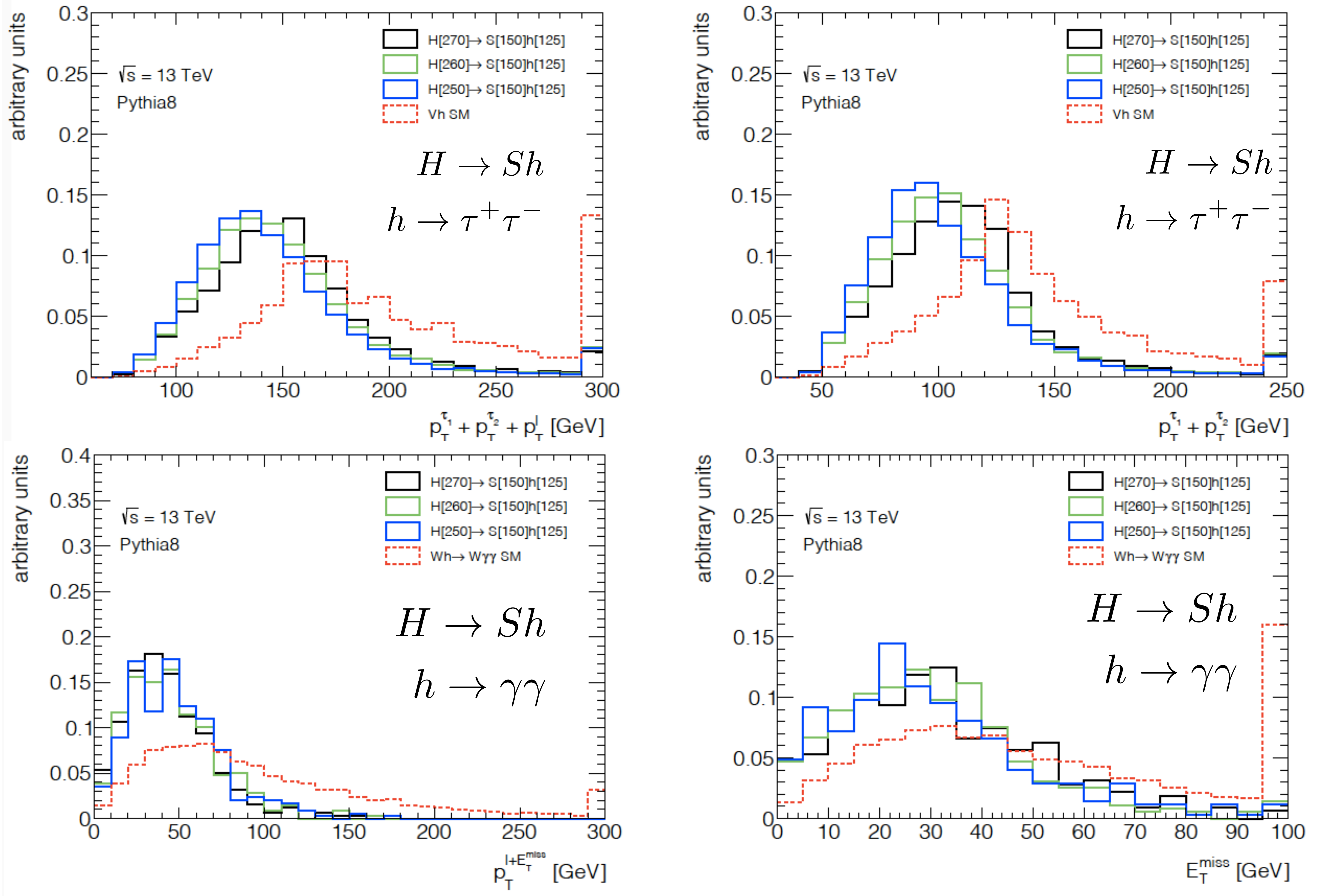

arbitrary units
√s = 13 TeV
Pythia8
H[270]→ S[150]h[125]
H[260]→ S[150]h[125]
H[250]→ S[150]h[125]
Vh SM
$H \to Sh$
$h \to \tau^+\tau^-$
$p_T^{\tau_1} + p_T^{\tau_2} + p_T^{l}$ [GeV]
arbitrary units
√s = 13 TeV
Pythia8
H[270]→ S[150]h[125]
H[260]→ S[150]h[125]
H[250]→ S[150]h[125]
Vh SM
$H \to Sh$
$h \to \tau^+\tau^-$
$p_T^{\tau_1} + p_T^{\tau_2}$ [GeV]
arbitrary units
√s = 13 TeV
Pythia8
H[270]→ S[150]h[125]
H[260]→ S[150]h[125]
H[250]→ S[150]h[125]
Wh→ Wγγ SM
$H \to Sh$
$h \to \gamma\gamma$
$p_T^{l+E_T^{miss}}$ [GeV]
arbitrary units
√s = 13 TeV
Pythia8
H[270]→ S[150]h[125]
H[260]→ S[150]h[125]
H[250]→ S[150]h[125]
Wh→ Wγγ SM
$H \to Sh$
$h \to \gamma\gamma$
E_T^{miss} [GeV]

Survey of LHC results on Vh (V=W,Z) production (Y. Hernandez et al., in preparation)

The BSM (H→Sh) signal appears at low p_{Th} and the SM signal is prevalent at larger p_{Th}

Include those results from ATLAS and CMS where no requirements on p_{Th} (or correlated observables) is not done or used in an MVA.

Those results where the final state is treated more "inclusively" display elevated signal strengths for Wh production.

$$\mu_{Inc}(Vh) = 2.51 \pm 0.43$$

This represents a 3.5σ deviation from the SM value of 1. BSM signal normalization less than expected from multilepton excesses assuming Br(H→Sh)=100%. Indicates that Br(H→SS) > Br(H→Sh)

TABLE I. Summary of ATLAS and CMS Vh results.

Higgs decay	Ref.	Experiment	$\sqrt{s}$	Final state	Category	μ	Used in combination	Comments
WW	[17]	ATLAS	7,8 TeV	2ℓ	DFOS 2j	$2.2^{+2.0}_{-1.9}$	✓	
					SS 1j	$8.4^{+4.3}_{-3.8}$	✓	2ℓ combination: $\mu = 3.7^{+1.9}_{-1.5}$
					SS 2j	$7.6^{+6.0}_{-5.4}$	✓	
				3ℓ	1SFOS	$-2.9^{+2.7}_{-2.1}$	x	$m_{\ell_0\ell_2}$ used as input BDT discriminating variable
					0SFOS	$1.7^{+1.9}_{-1.4}$	✓	
	[18]	ATLAS	13 TeV	3ℓ	1SFOS 0SFOS	$2.3^{+1.2}_{-1.0}$	✓	1SFOS channel uses $m_{\ell_0\ell_2}$ in the BDT but excess driven by 0SFOS
	[19]	CMS	7,8 TeV	2ℓ	DFOS 2j	$0.39^{+1.97}_{-1.87}$	✓	Discrepancy at low $m_{\ell\ell}$
				3ℓ	0+1SFOS	$0.56^{+1.27}_{-0.95}$	✓	
	[20]	CMS	13 TeV	2ℓ	DFOS 2j	$3.92^{+1.32}_{-1.17}$	✓	Discrepancy at low $m_{\ell\ell}$
				3ℓ	0+1SFOS	$2.23^{+1.76}_{-1.53}$	✓	
$\tau\tau$	[21]	ATLAS	7,8 TeV	1ℓ	$\ell + \tau_h\tau_h$	1.8 ± 3.1	✓	
				2ℓ	$e^{\pm}\mu^{\pm} + \tau_h$	1.3 ± 2.8	✓	
	[22]	CMS	7,8 TeV	1ℓ	$\ell + \tau_h\tau_h$	-0.33 ± 1.02	x	BDT based on $p_T^{\tau_1} + p_T^{\tau_2}$
				2ℓ	$e^{\pm}\mu^{\pm} + \tau_h$		x	Split $p_T^{\ell_1} + p_T^{\ell_2} + p_T^{\tau}$ at 130 GeV
	[23]	CMS	13 TeV	1ℓ	$\ell + \tau_h\tau_h$	$3.39^{+1.68}_{-1.54}$	✓	
				2ℓ	$e^{\pm}\mu^{\pm} + \tau_h$			
$\gamma\gamma$	[24]	ATLAS	7,8 TeV	$\ell\nu$	one-lepton	1.0 ± 1.6	x	
				$\ell\ell,\nu\nu$	E_T^{miss}			$E_T^{miss} > 70 - 100$ GeV
				jj	Hadronic			$p_{Tt}^{\gamma\gamma} > 70$ GeV
	[26]	CMS	7,8 TeV	$\ell\nu$	one-lepton	-0.16 ± 0.97	x	Split E_T^{miss} at 45 GeV
				$\ell\ell,\nu\nu$	E_T^{miss}			$E_T^{miss} > 70$ GeV
				jj	Hadronic			$p_T^{\gamma\gamma} > 13m_{\gamma\gamma}/12$
	[25]	ATLAS	13 TeV	$\ell\nu$	one-lepton	$0.7^{+0.9}_{-0.8}$	x	$p_T^{\ell+E_T^{miss}} > 150$ GeV $p_T^{\ell+E_T^{miss}} < 150$ GeV
				$\ell\ell,\nu\nu$	E_T^{miss}			$150 < E_T^{miss} < 250$ GeV $80 < E_T^{miss} < 150$ GeV
				jj	Hadronic			BDT used based on m_{jj} and $p_{Tt}^{\gamma\gamma}$
	[27]	CMS	13 TeV	$\ell\nu$	one-lepton	$2.4^{+1.1}_{-1.0}$	✓	Split E_T^{miss} at 45 GeV ($\mu = 3.0^{+1.5}_{-1.3}$)
				$\ell\ell,\nu\nu$	E_T^{miss}		x	$E_T^{miss} > 85$ GeV
				jj	Hadronic		✓	$p_T^{\gamma\gamma}/m_{\gamma\gamma}$ not used ($\mu = 5.1^{+2.5}_{-2.3}$)

Eur.Phys.J. C76 (2016) no.10, 580

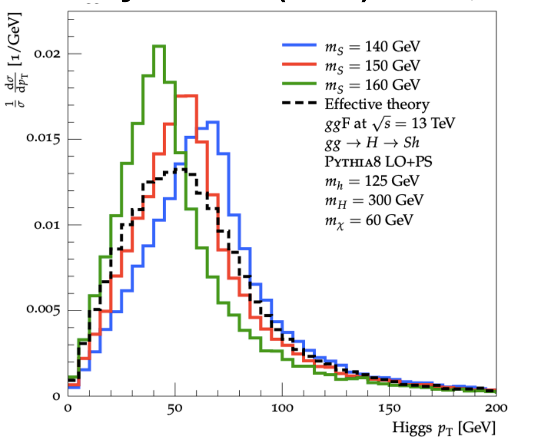

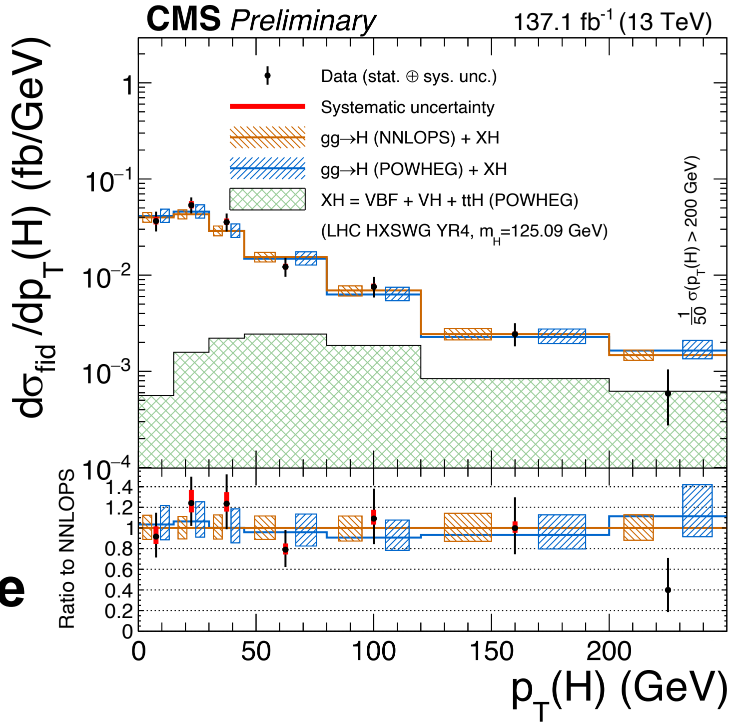

CMS-PAS-HIG-19-001

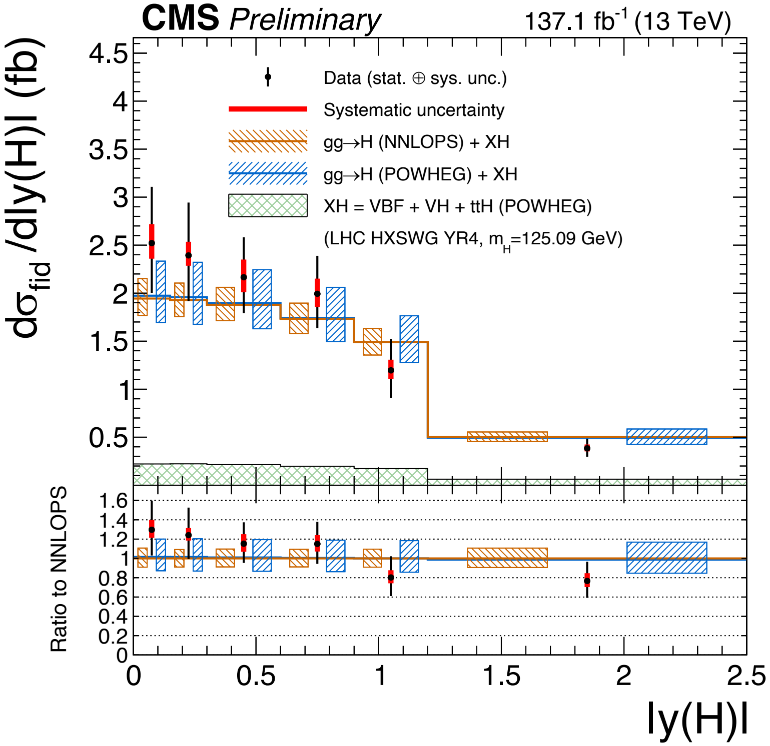

Simplified model predicts low p_{Th}. Due to proximity of the turnover, uncertainties are hard to assess.

Working with IHEP and V. Ravindran et al. to evaluate robustness of rapidity, where data tends to be more central than prediction

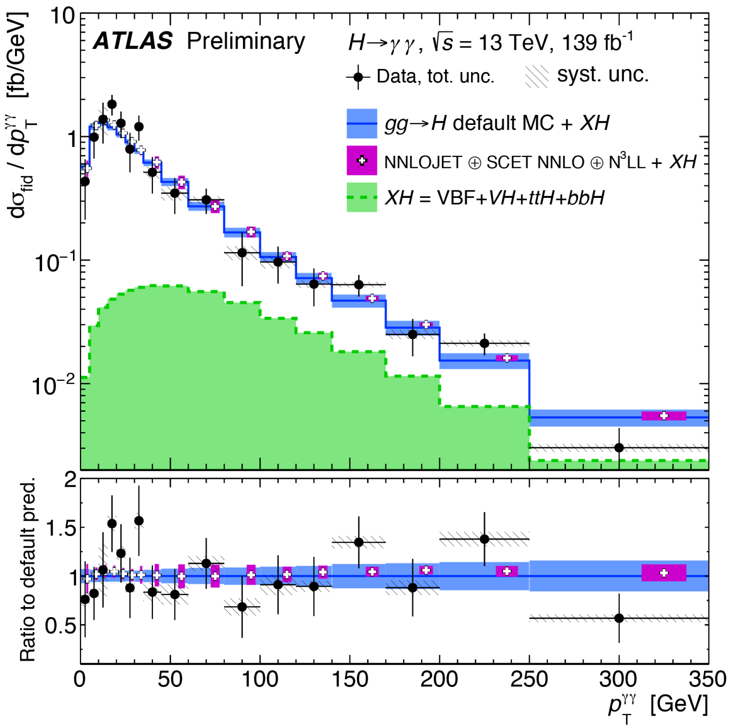

ATLAS-CONF-2019-029

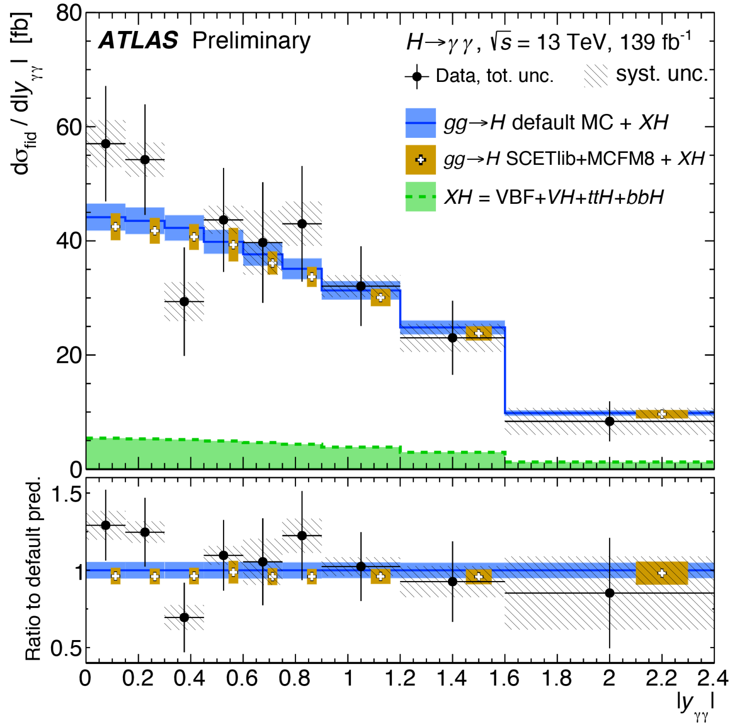

V. Ravindran et al.

- F.O. and resummed results for few benchmark values of y

y	LO	LO + LL	NLO	NLO + NLL	NNLO	NNLO + NNLL	NNLO + NNNLL
0.0	4.435 ± 1.145	6.231 ± 1.950	8.255 ± 1.684	9.632 ± 2.286	10.329 ± 1.088	10.938 ± 1.050	10.517 ± 0.820
0.8	4.134 ± 1.067	5.833 ± 1.831	7.517 ± 1.530	8.820 ± 2.124	9.407 ± 0.988	9.992 ± 1.025	9.641 ± 0.718
1.6	3.189 ± 0.819	4.630 ± 1.468	5.522 ± 1.117	6.611 ± 1.676	6.877 ± 0.744	7.380 ± 0.849	7.045 ± 0.563
2.4	1.904 ± 0.492	2.887 ± 0.942	2.985 ± 0.597	$3.715 \pm .998$	3.683 ± 0.410	4.040 ± 0.501	3.821 ± 0.305

Banerjee, Das, Dhani, Ravindran ('17)

- Corrections from LL varies between **40%** to **50%** from LO.
- At NLL it is **17%** to **24%**;
- At NNLL **6%** to **10%**.
- NNLO+NNNLL **3%** to **5%**.

Scale uncertainty goes down 12% to 6% at NNLO+N3LL

- **The result can be further improved with known NNNLO corrections.**

Ajjath, Chen, Cieri, Das, Gehrmann, Mukherjee, Ravindran (in preparation)

Outlook and Conclusions

- Discrepancies in multi-lepton final states at the LHC with current MC tools are strong
  - While significance is dominated by OS di-lepton final states, discrepancies appear in SS ll and 3l
  - They appear in corners of the phase-space dominated by different processes: Wt/tt, WW, ZW
    - Hard to explain with mismodelling of one process
- Discrepancies interpreted with simplified model where H→Sh, S is treated as SM Higgs-like and one parameter is floated
- Features of the Higgs data from LHC agree qualitatively with the simplified model used here
- Further strengthens the need for precise measurement of Higgs couplings in e^+e^- (and ep)

Additional Slides

The Lagrangian

arXiv:1506.00612
arXiv:1603.01208
arXiv:1606.01674

Introduce H and X fields with the interactions listed below

$$\mathcal{L} = \mathcal{L}_{SM} + \mathcal{L}_{BSM}$$

$$\mathcal{L}_{BSM} = \mathcal{L}_{K} + \mathcal{L}_{T} + \mathcal{L}_{Q} + \mathcal{L}_{Hgg} + \mathcal{L}_{HVV}$$

$$\mathcal{L}_{K} = \frac{1}{2}\partial_\mu X \partial^\mu X + \frac{1}{2}\partial_\mu H \partial^\mu H - \frac{1}{2}M_X^2 X^2 - \frac{1}{2}M_H^2 H^2$$

$$\mathcal{L}_{T} = -\frac{1}{2}\mu_1 h^2 H - \frac{1}{2}\mu_2 X^2 h - \frac{1}{2}\mu_3 X^2 H$$

$$\mathcal{L}_{Q} = -\frac{1}{4}\lambda_1 H^2 h^2 - \frac{1}{4}\lambda_2 X^2 h^2 - \frac{1}{4}\lambda_3 H^2 X^2 - \frac{1}{2}\lambda_4 H h X^2$$

$$\mathcal{L}_{Hgg} = -\frac{1}{4}\beta_g \ \kappa_{hgg}^{SM} G_{\mu\nu} G^{\mu\nu} H$$

$$\mathcal{L}_{HVV} = \frac{2M_W^2}{v}\beta_W \ W_\mu W^\mu H + \frac{M_Z^2}{v}\beta_Z \ Z_\mu Z^\mu H$$

The Lagrangian

Can be embedded into 2HDM+S (N2HDM)
See also M.Muhlleitner et al.
arXiv:1612.01309
arXiv:1708.01578

$$\mathcal{L}_K = \frac{1}{2}\partial_\mu S \partial^\mu S - \frac{1}{2} m_S^2 SS,$$

$$\mathcal{L}_{SVV'} = \frac{1}{4}\kappa_{Sgg}\frac{\alpha_s}{12\pi v} S G^{a\mu\nu} G^a_{\mu\nu} + \frac{1}{4}\kappa_{S\gamma\gamma}\frac{\alpha}{\pi v} S F^{\mu\nu} F_{\mu\nu} + \frac{1}{4}\kappa_{SZZ}\frac{\alpha}{\pi v} S Z^{\mu\nu} Z_{\mu\nu} + \frac{1}{4}\kappa_{SZ\gamma}\frac{\alpha}{\pi v} S Z^{\mu\nu} F_{\mu\nu} + \frac{1}{4}\kappa_{SWW}\frac{2\alpha}{\pi s_w^2 v} S W^{+\mu\nu} W^-_{\mu\nu},$$

$$\mathcal{L}_{Sf\bar{f}} = -\sum_f \kappa_{Sf}\frac{m_f}{v} S\bar{f}f,$$

$$\mathcal{L}_{HhS} = -\frac{1}{2}\, v\left[\lambda_{hhS} hhS + \lambda_{hSS} hSS + \lambda_{HHS} HHS + \lambda_{HSS} HSS + \lambda_{HhS} HhS\right],$$

$$\mathcal{L}_{S\chi} = -\frac{1}{2}\, v\, \lambda_{S\chi\chi} S\chi\chi - \frac{1}{2}\lambda_{SS\chi\chi} SS\chi\chi.$$

$$\mathcal{L}_S = \mathcal{L}_K + \mathcal{L}_{SVV'} + \mathcal{L}_{Sf\bar{f}} + \mathcal{L}_{hHS} + \mathcal{L}_{S\chi}$$

Note that some of the effective quartic couplings shown earlier appear here as trilinear.
What was formerly a three body decay is now a two body decay.

The Decays of H

- In the general case, H can have couplings as those displayed by a Higgs boson in addition to decays involving the intermediate scalar and Dark Matter

$$H \to WW, ZZ, q\bar{q}, gg, Z\gamma, \gamma\gamma, \chi\chi$$

$$+ \quad H \to SS, Sh, hh$$

Dominant decays

Diboson decay

$$H \to h(+X), S(+X)$$

The intermediate scalar, S

- Dark Matter is introduced in the form of a scalar and the decay H→h\chi\chi via effective quartic couplings

$$\mathcal{L}_{\rm Q} = -\frac{1}{2}\lambda_{Hh\chi\chi} H h \chi\chi - \frac{1}{4}\lambda_{HHhh} H H h h - \frac{1}{4}\lambda_{hh\chi\chi} h h \chi\chi - \frac{1}{4}\lambda_{HH\chi\chi} H H \chi\chi$$

- Due to gauge invariance we encounter an awkward situation where a three body decay may be larger or comparable to a two body decay. This can be naturally explained by introducing an intermediate real scalar S

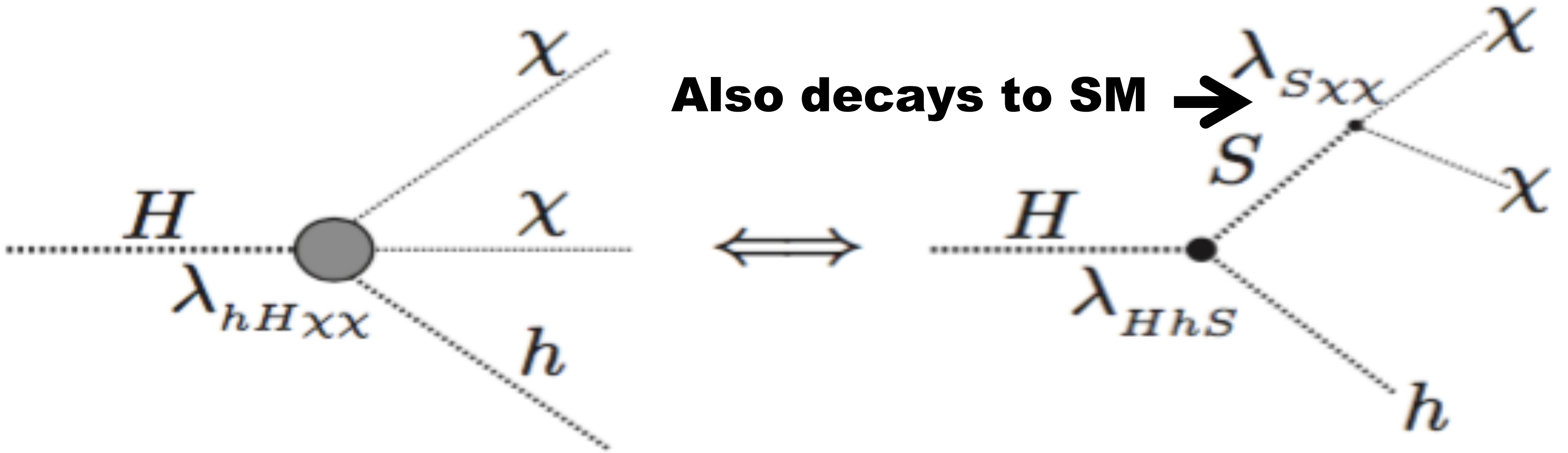

Masses in the 2HDM+S

$$\begin{pmatrix} H_1 \\ H_2 \\ H_3 \end{pmatrix} = \mathbb{R} \begin{pmatrix} \rho_1 \\ \rho_2 \\ \rho_S \end{pmatrix},$$

Mass-matrix for the CP-even scalar sector will modified with respect to 2HDM and that needs a 3 x3 matrix (three mixing angles). Couplings are modified.

$$\mathbb{R} = \begin{pmatrix} c_{\alpha_1} c_{\alpha_2} & s_{\alpha_1} c_{\alpha_2} & s_{\alpha_2} \\ -(c_{\alpha_1} s_{\alpha_2} s_{\alpha_3} + s_{\alpha_1} c_{\alpha_3}) & c_{\alpha_1} c_{\alpha_3} - s_{\alpha_1} s_{\alpha_2} s_{\alpha_3} & c_{\alpha_2} s_{\alpha_3} \\ -c_{\alpha_1} s_{\alpha_2} s_{\alpha_3} + s_{\alpha_1} s_{\alpha_3} & -(c_{\alpha_1} s_{\alpha_3} + s_{\alpha_1} s_{\alpha_2} c_{\alpha_3}) & c_{\alpha_2} c_{\alpha_3} \end{pmatrix}$$

$$M^2_{\mathrm{CP-even}} = \begin{pmatrix} 2\lambda_1 v_1^2 - m_{12}\frac{v_2}{v_1} & m_{12} + \lambda_{345} v_1 v_2 & 2\kappa_1 v_1 v_S \\ m_{12} + \lambda_{345} v_1 v_2 & -m_{12}\frac{v_2}{v_1} + 2\lambda_2 v_2^2 & 2\kappa_2 v_2 v_S \\ 2\kappa_1 v_1 v_S & 2\kappa_2 v_2 v_S & \frac{1}{3}\lambda_S v_S^2 \end{pmatrix}$$

$$
\begin{aligned}
m_{H_1}^2 &= v_S \sin\alpha_2 \left[\lambda_7 v \cos\alpha_1 \cos\alpha_2 \cos\beta + \lambda_8 v \sin\alpha_1 \cos\alpha_2 \sin\beta + \lambda_6 v_S \sin\alpha_2\right], \\
m_{H_2}^2 &= (\cos\alpha_1 \cos\alpha_3 - \sin\alpha_1 \sin\alpha_2 \sin\alpha_3) \Big[\cos\alpha_1 \cos\alpha_2 \left(\lambda_{345} v^2 \sin\beta\cos\beta - m_{12}^2\right) \\
&\quad + \sin\alpha_1 \cos\alpha_2 \left(m_{12}^2 \cot\beta + \lambda_2 v^2 \sin^2\beta\right) + \lambda_8 v v_S \sin\alpha_2 \sin\beta\Big], \\
m_{H_3}^2 &= (\sin\alpha_1 \sin\alpha_3 - \sin\alpha_2 \cos\alpha_1 \cos\alpha_3) \Big[\cos\alpha_1 \cos\alpha_2 \left(m_{12}^2 \tan\beta + \lambda_1 v^2 \cos^2\beta\right) \\
&\quad + \sin\alpha_1 \cos\alpha_2 \left(\lambda_{345} v^2 \sin\beta\cos\beta - m_{12}^2\right) + \lambda_7 v v_S \sin\alpha_2 \cos\beta\Big]. \qquad (2.17)
\end{aligned}
$$

Perform scans after fixing masses of physical bosons(m_{h1}=125 GeV, m_{h2}=140, m_{h3}=270 GeV, m_A=600 GeV, $m_H\pm$=600 GeV) in addition to the constraints described in arXiv:1711.07874, including the signal Yukawa coupling strength of β_g^2=1.38±0.22 (translated into $\tan^2\beta$)

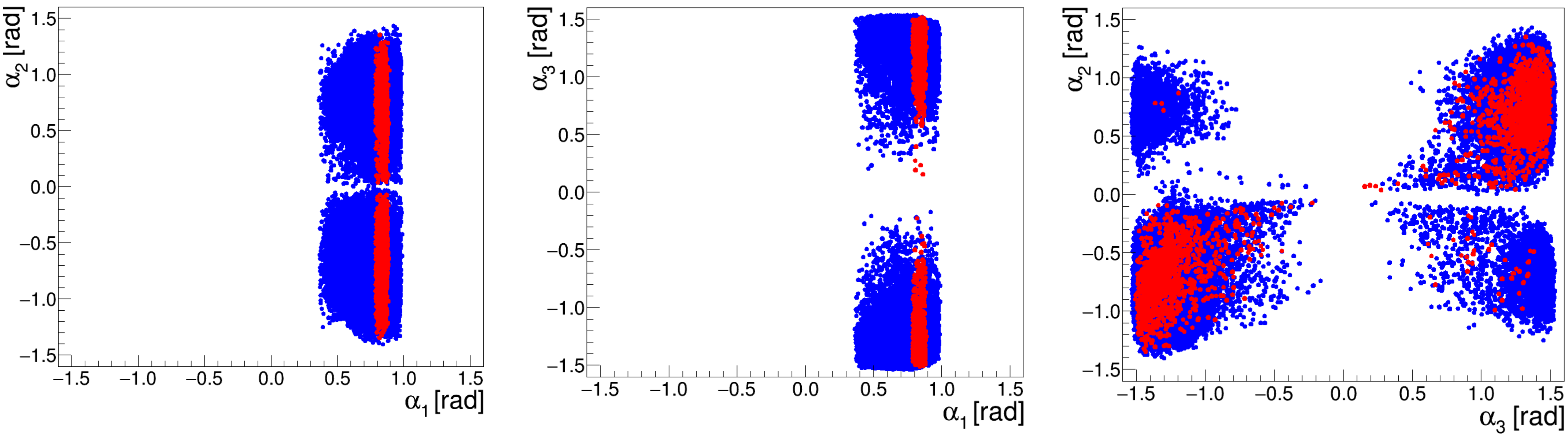

Correlation plots for the three mixing angles and tanβ. Blue (red) points correspond to Br(h→SM) within 10% (20%) of the SM h values (arXiv:1809.06344)

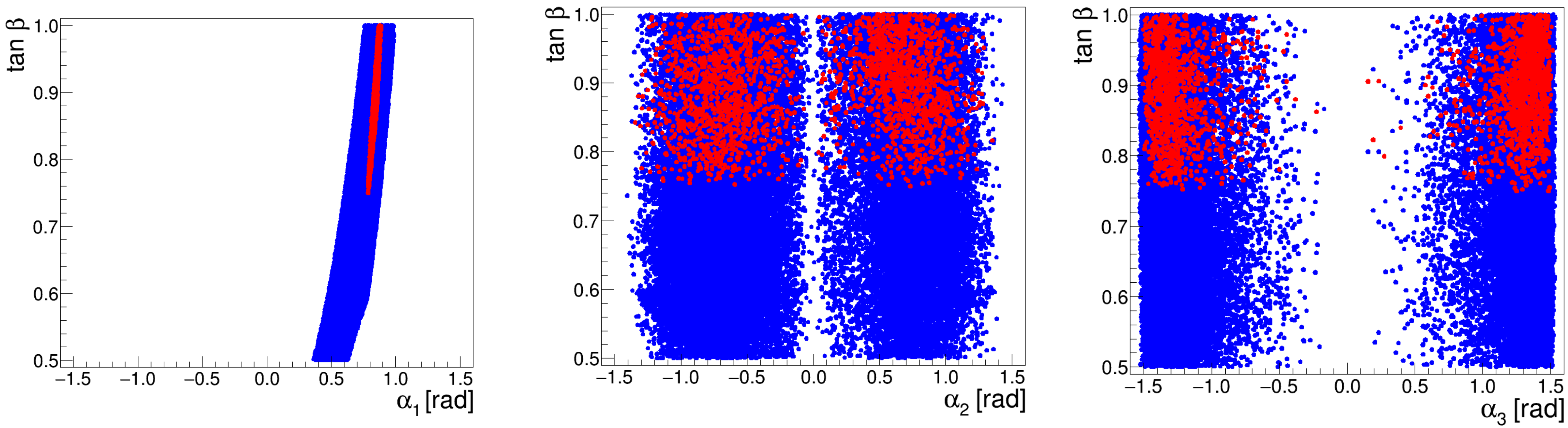

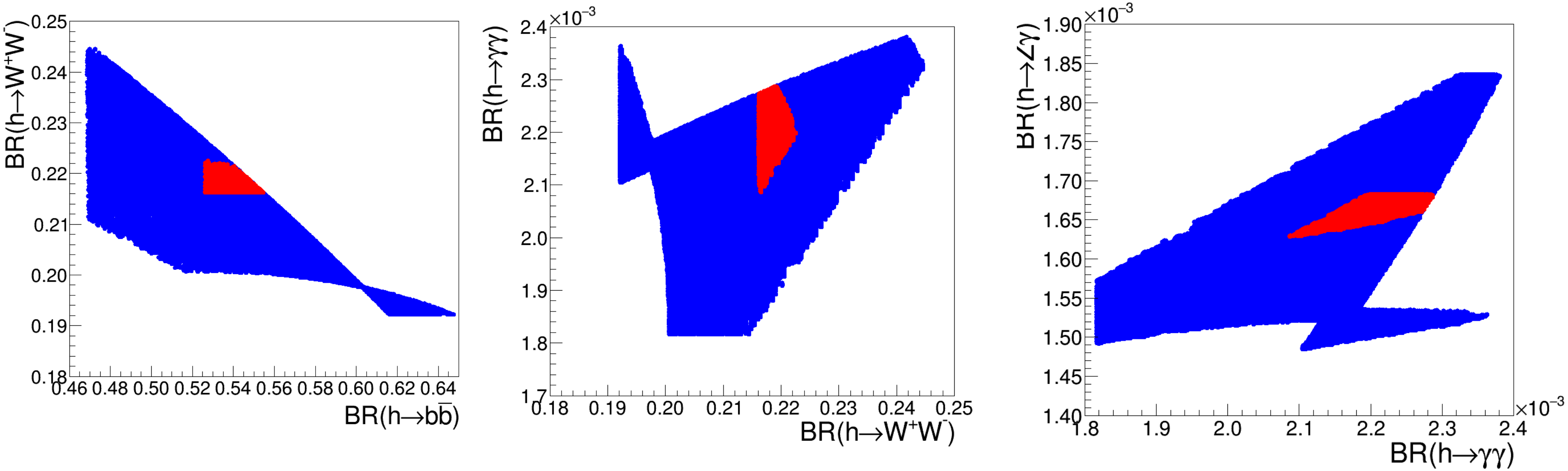

Results using N2HDECAY (arXiv:1612.01309) for one benchmark point

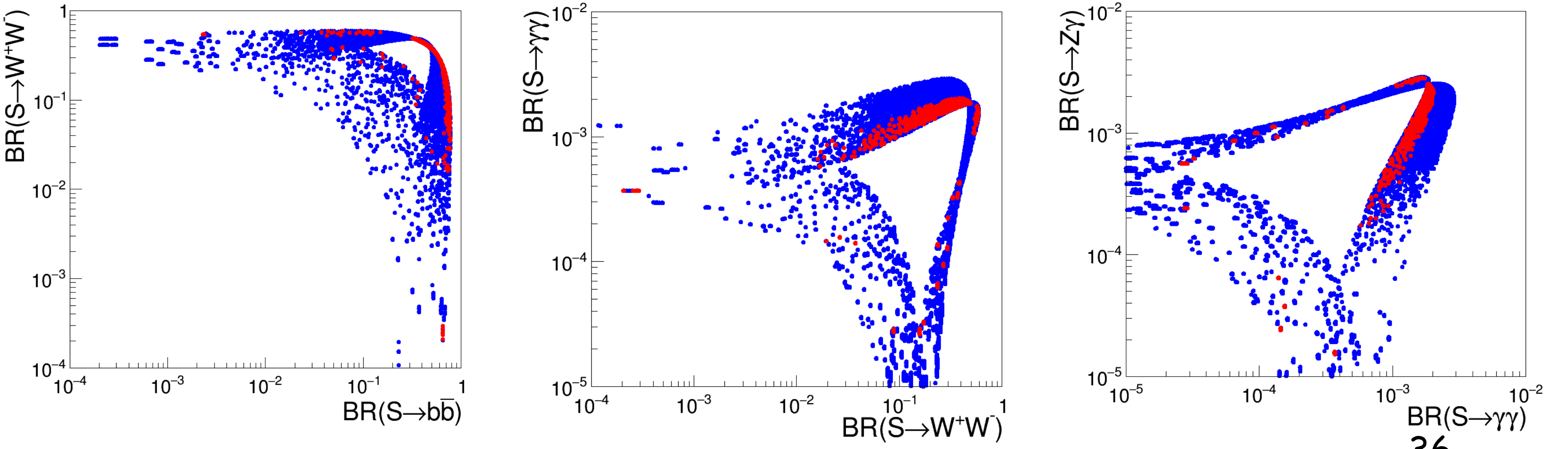

For simplicity we will assume that the S decays like the SM Higgs boson

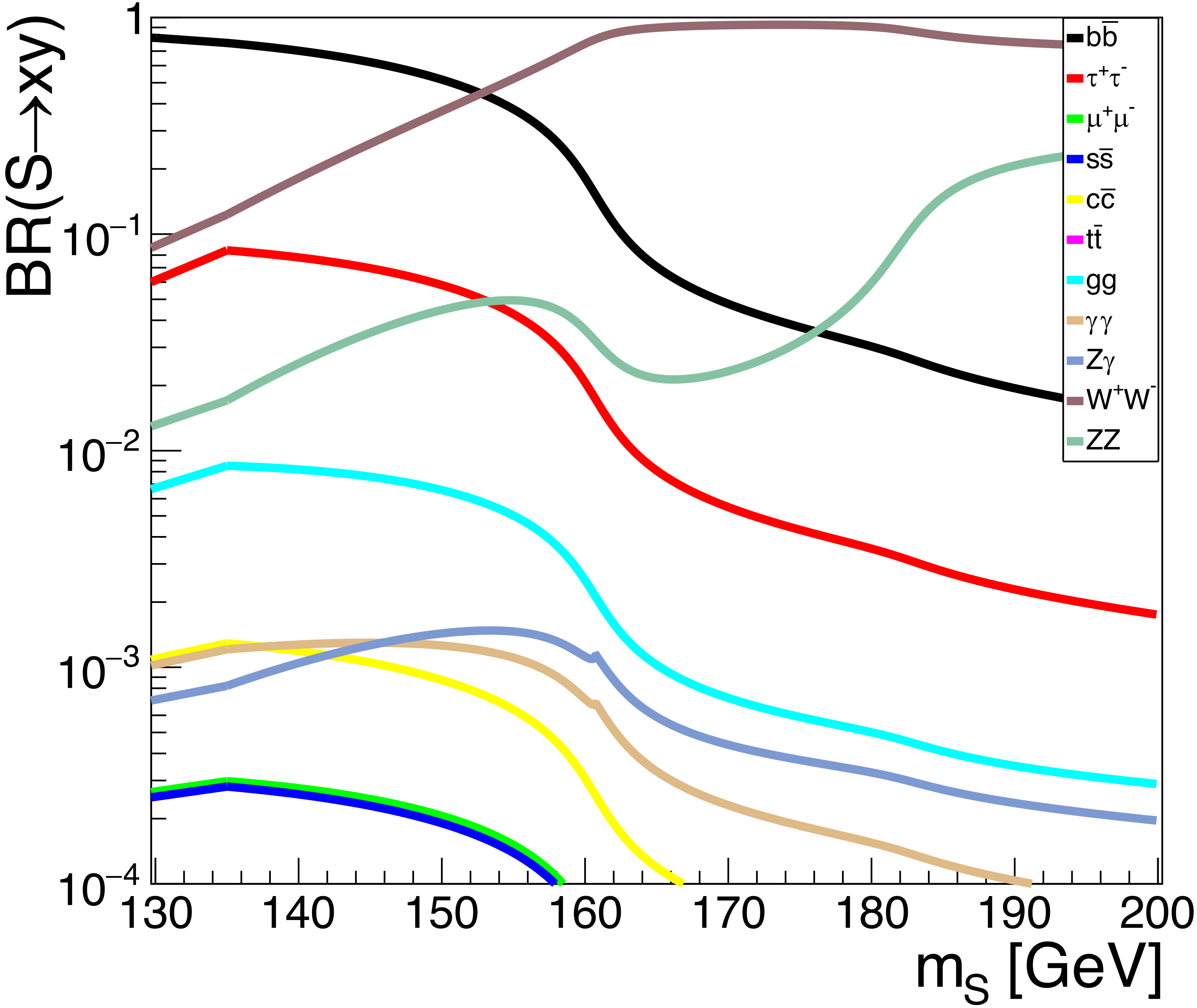

Impact on h boson measurements

- The most prominent feature pertains to additional production mechanism (i.e. H→Sh) of h with large jet activity (from S→jets, model dependency). Expect distortion of the p_T spectrum, as well.

- At this point we are studying the contamination of the H→Sh production mechanism on measurement with hadronic final states: h+≥2j, VBF, V(→jj)h, Vh(→bb) (not discussed here) h signal strengths

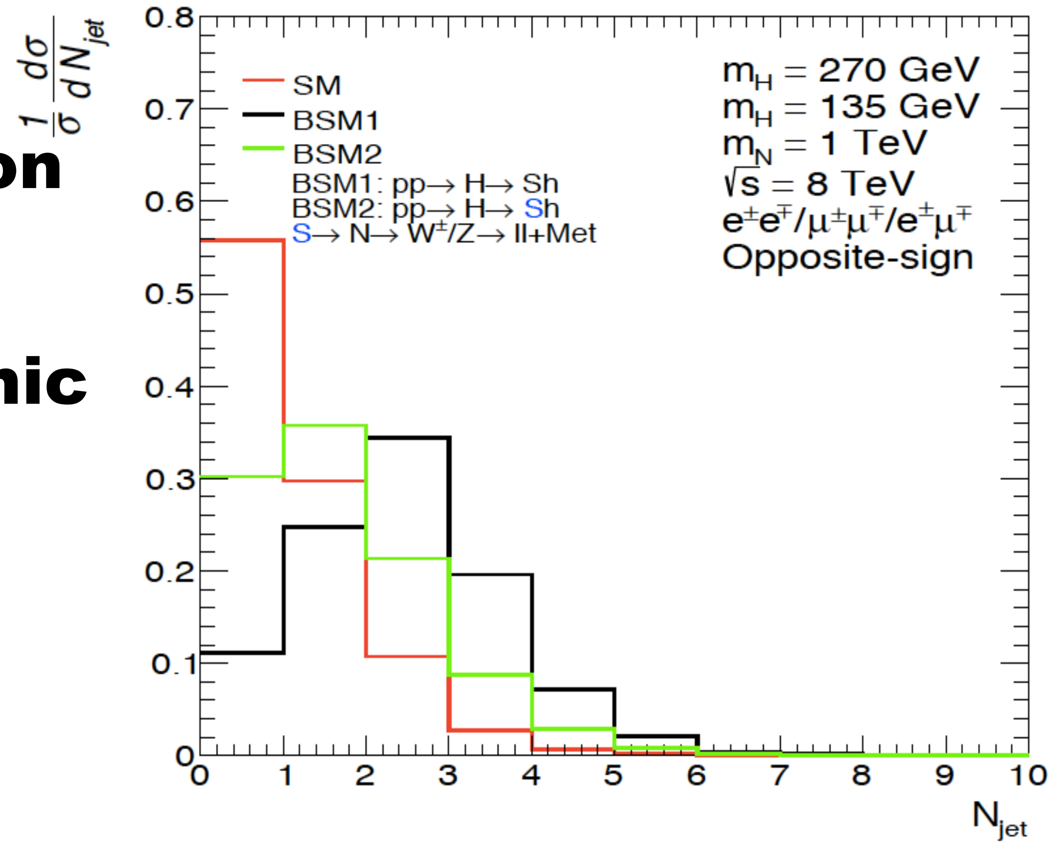

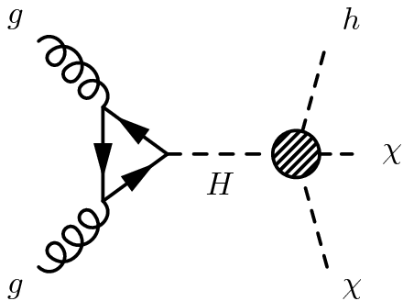

ATLAS, arXiv:1706.03948

Limits on h(→γγ)+MET

Category	Requirements
Mono-Higgs	$S_{E_T^{miss}} > 7\ \sqrt{\text{GeV}}$, $p_T^{\gamma\gamma} > 90$ GeV, lepton veto
High-E_T^{miss}	$S_{E_T^{miss}} > 5.5\ \sqrt{\text{GeV}}$, $\lvert z_{PV}^{highest} - z_{PV}^{\gamma\gamma}\rvert < 0.1$ mm
Intermediate-E_T^{miss}	$S_{E_T^{miss}} > 4\ \sqrt{\text{GeV}}$, $p_T^{hard} > 40$ GeV , $\lvert z_{PV}^{highest} - z_{PV}^{\gamma\gamma}\rvert < 0.1$ mm
Different-Vertex	$S_{E_T^{miss}} > 4\ \sqrt{\text{GeV}}$, $p_T^{hard} > 40$ GeV , $\lvert z_{PV}^{highest} - z_{PV}^{\gamma\gamma}\rvert > 0.1$ mm
Rest	$p_T^{\gamma\gamma} > 15$ GeV

$$S_{E_T^{miss}} = E_T^{miss} / \sqrt{\sum E_T}$$

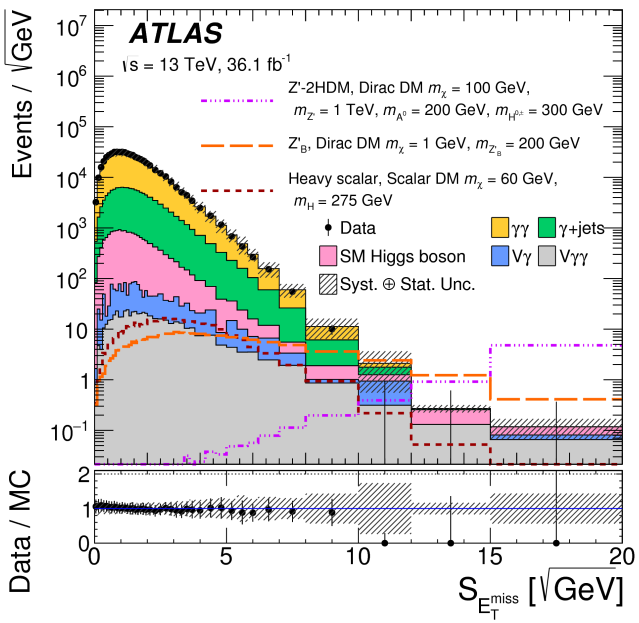

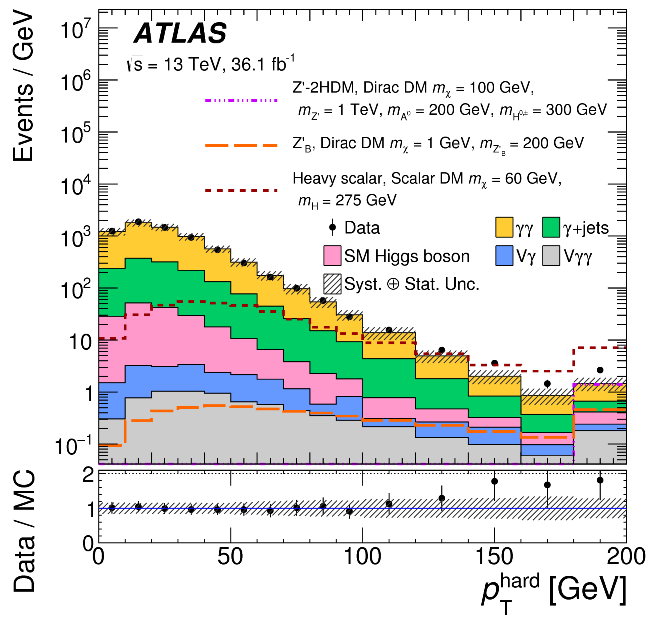

ATLAS, arXiv:1706.03948

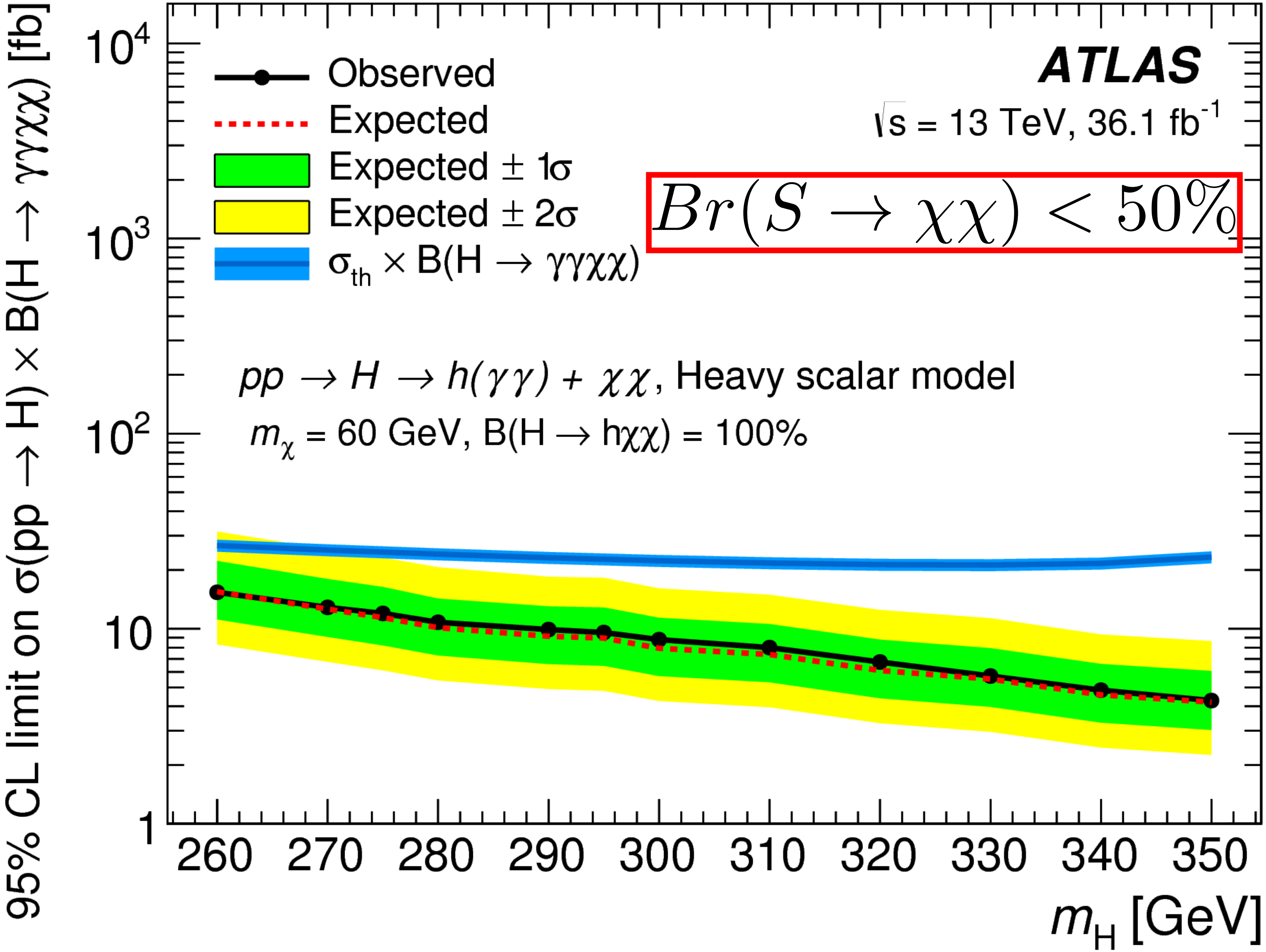

Enhancement of tH production

- **In experiment, top associated Higgs production is measured as a sum of single top and double top cross sections**
- **In the SM, we find that $\sigma_{th} \ll \sigma_{tth}$**

$$\mathcal{A} = \frac{g}{\sqrt{2}}\left[(c_F - c_V)\frac{m_t\sqrt{s}}{m_W v} A\left(\frac{t}{s},\varphi;\xi_t,\xi_b\right) + \left(c_V\,\frac{2m_W}{v}\frac{s}{t} + (2c_F - c_V)\,\frac{m_t^2}{m_W v}\right) B\left(\frac{t}{s},\varphi;\xi_t,\xi_b\right)\right]$$

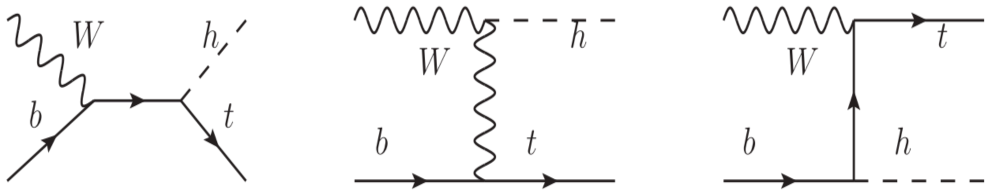

- **For the heavy scalar considered here, $c_V \ll c_F$**
- **We expect a sizeable cross section to come from top associated heavy scalar production ($\sigma_{tH} \simeq \sigma_{ttH}$)**

M. Farina, C. Grojean, F. Maltoni, E. Salvioni and A. Thamm, JHEP **1305**, 022 (2013).

Eur. Phys. J. C 77 (2017) 804

$$p_{T\ell} > 25\,\mathrm{GeV}$$

$$p_{Tb} > 25\,\mathrm{GeV}$$

$$N_{bjet} \geq 1$$

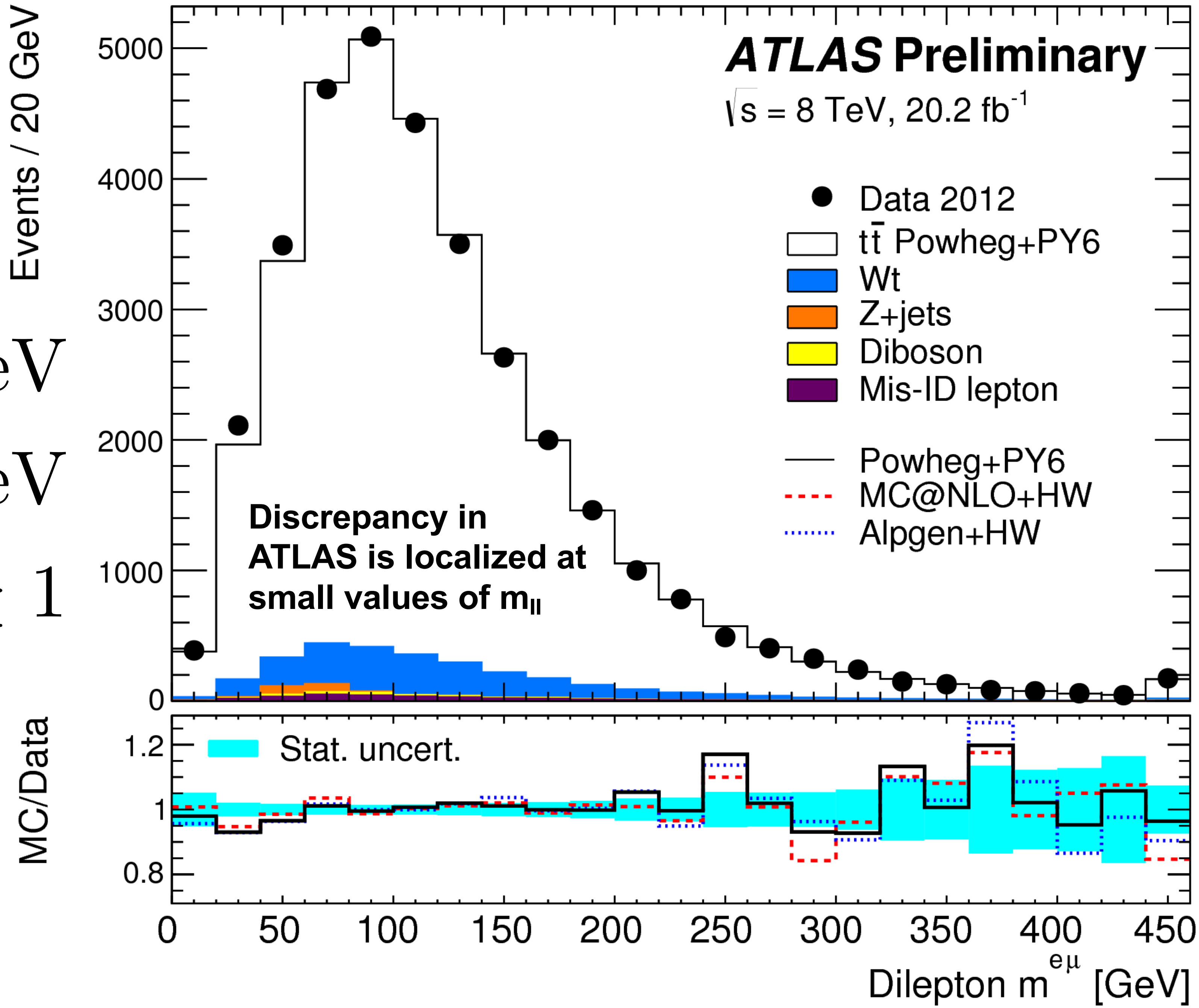

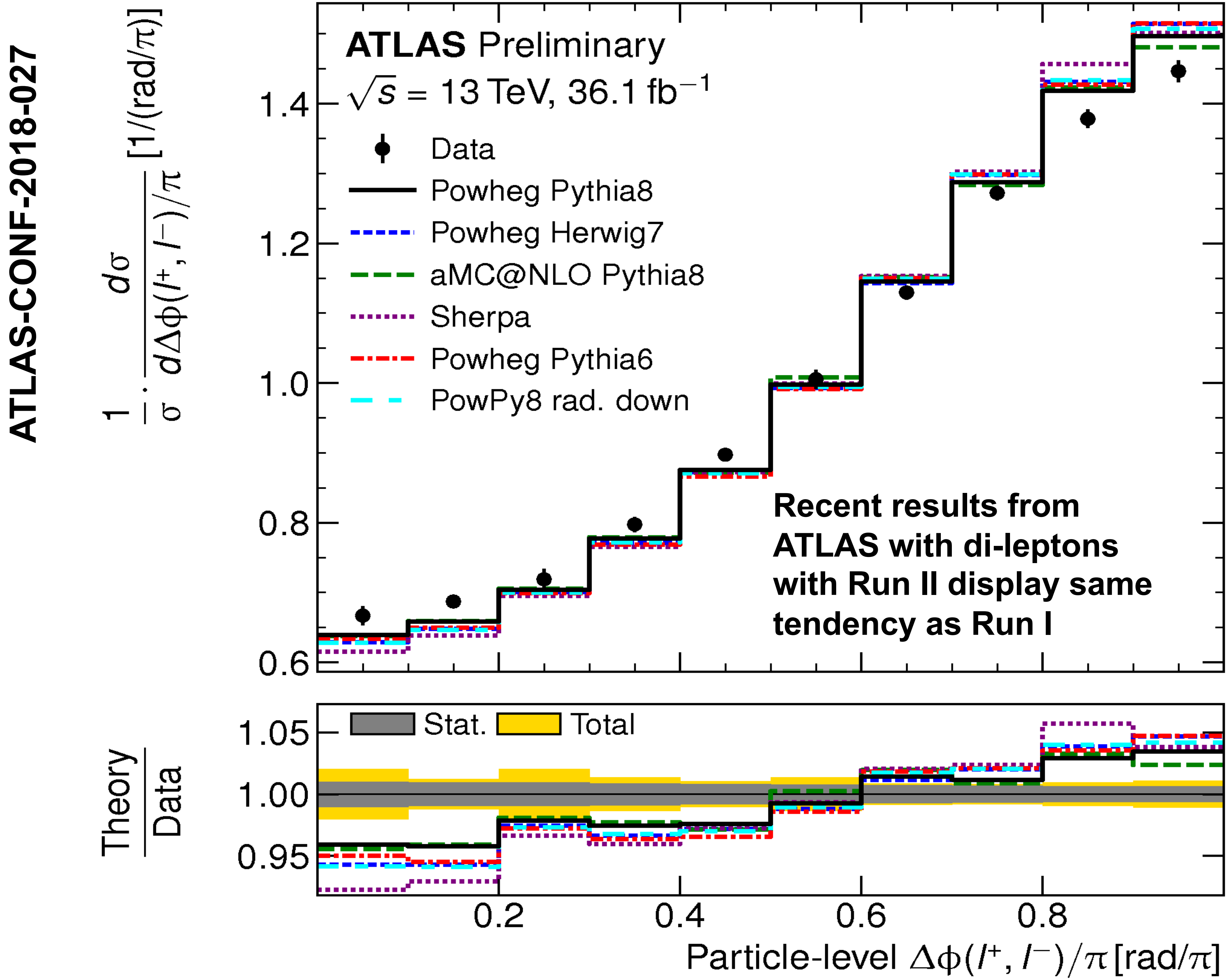
ATLAS-CONF-2018-027
ATLAS Preliminary
$\sqrt{s}$ = 13 TeV, 36.1 fb^{-1}
Data
Powheg Pythia8
Powheg Herwig7
aMC@NLO Pythia8
Sherpa
Powheg Pythia6
PowPy8 rad. down
Recent results from ATLAS with di-leptons with Run II display same tendency as Run I
$\frac{1}{\sigma} \cdot \frac{d\sigma}{d\Delta\phi(l^+,l^-)/\pi}$ [1/(rad/π)]
Stat.
Total
Theory / Data
Particle-level $\Delta\phi(l^+,l^-)/\pi$ [rad/π]

Fit results: ATLAS-CONF-2018-027

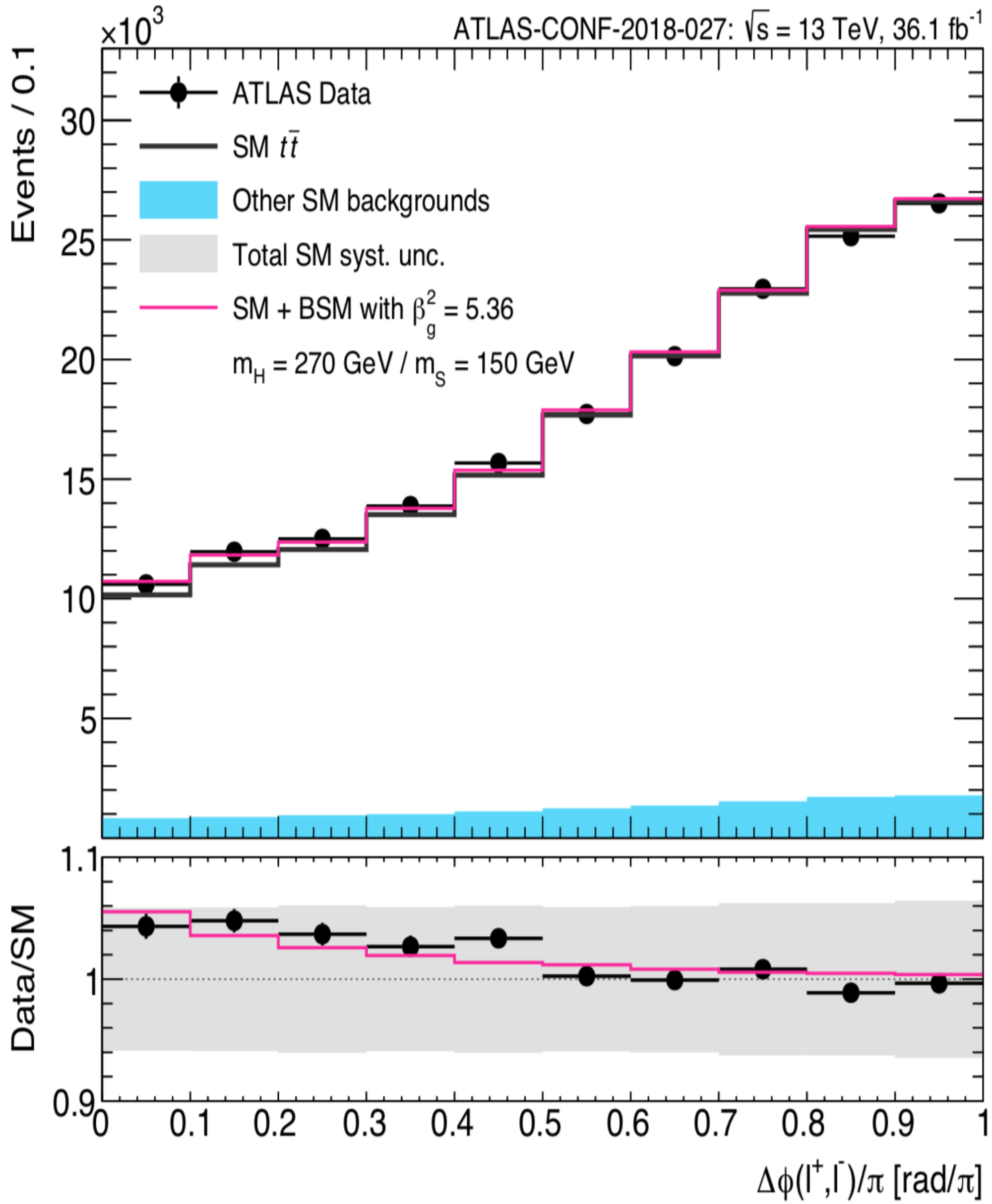

Simple selection:

- One DFOS lepton pair
- At least 1 *b*-tagged jet

Normalisation systematic: ~6.2%

Shape systematic:

- Discrepancy of SM prediction, particularly at high ΔΦ
- Choose SM prediction that best describes data (aMC@NLO) → systematic is percentage deviation away from mean SM prediction
- Varies between 1% and 2.6%

Fit results:

- $\beta_g^2 = 5.36 \pm 1.31$
- Somewhat higher, NNLO corrections can potentially help

What is the impact of NNLO QCD?

arXiv:1901.05407

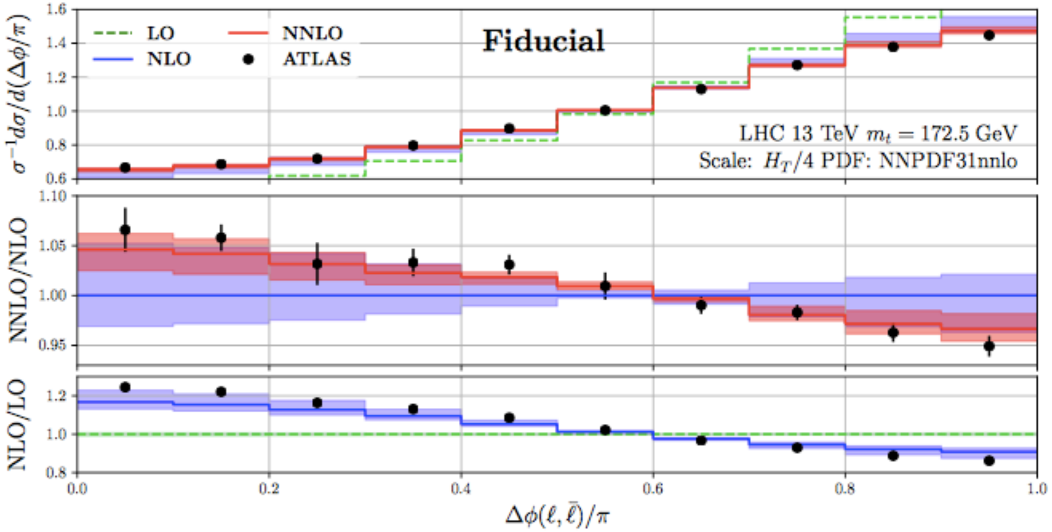

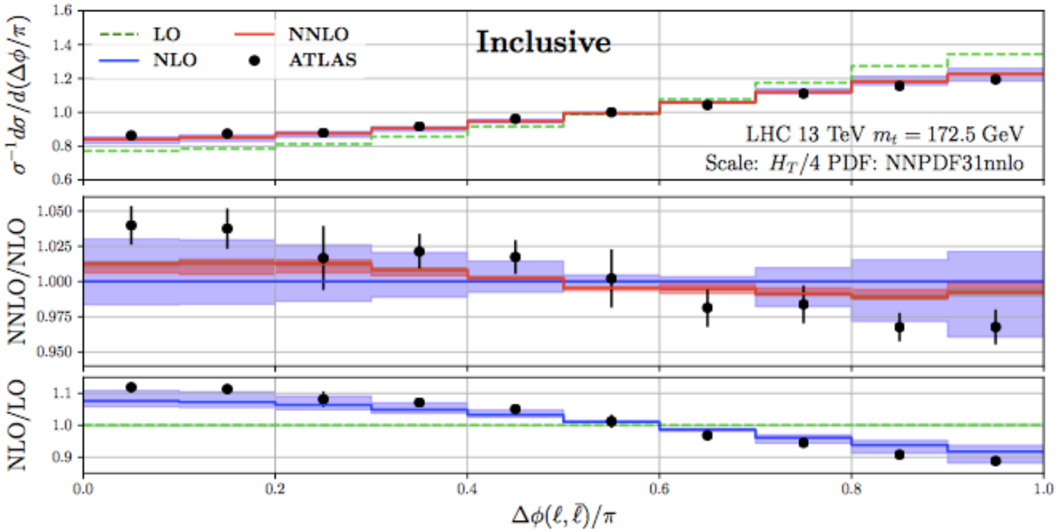

First look at the NNLO QCD corrections for the azimuthal angle difference of two leptons in tt production. Discrepancy is alleviated. By contrast the NNLO QCD corrections will push m_{ll} to higher values, increasing the excess in the m_{ll} distribution. <u>**This helps with the internal consistency of the BSM interpretation bringing the normalization of both excesses together**</u>

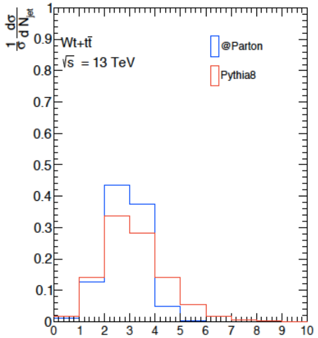

Study with POWHEG's NLO ME with and without PS, which adds jets in the final state. The correlation is such that is lowered and $\Delta\varphi_{ll}$ and m_{ll} is increased.

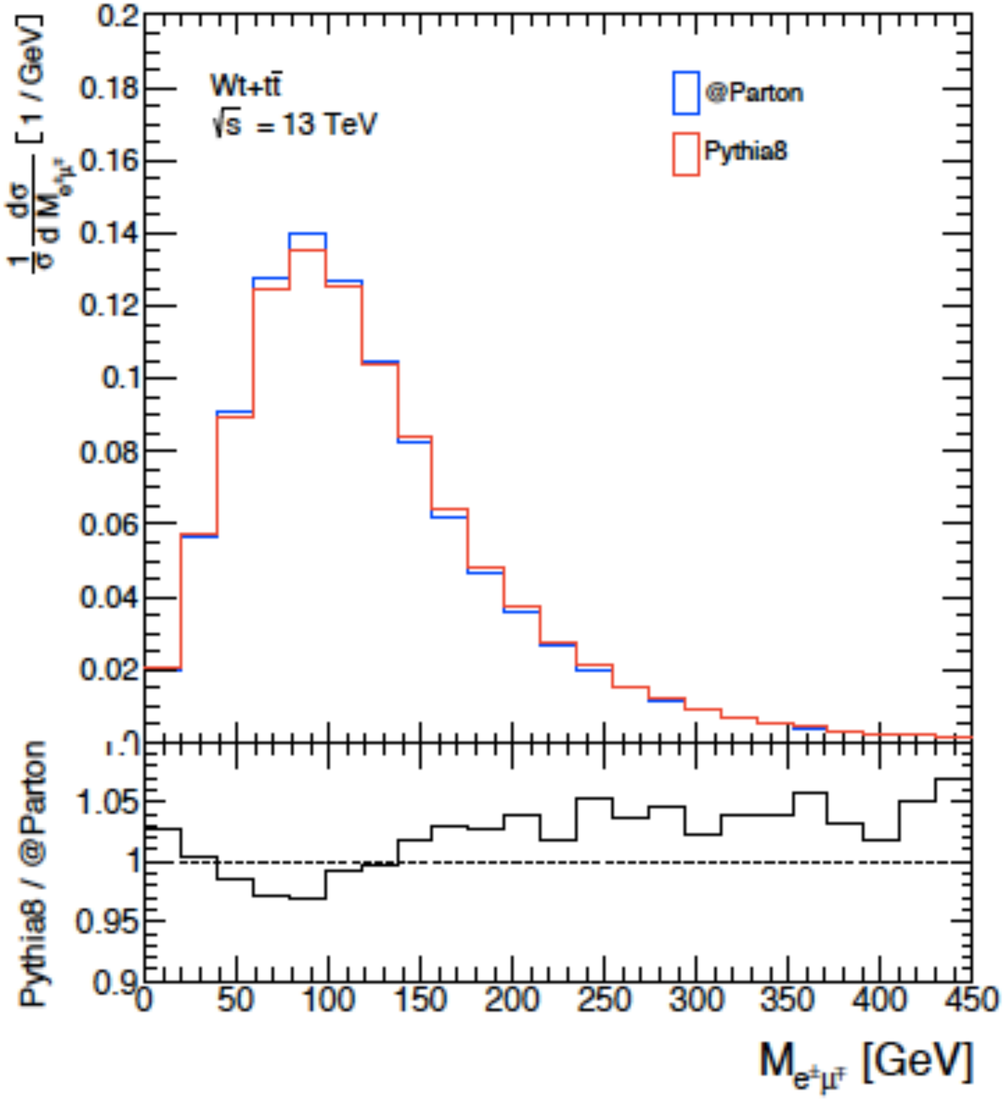

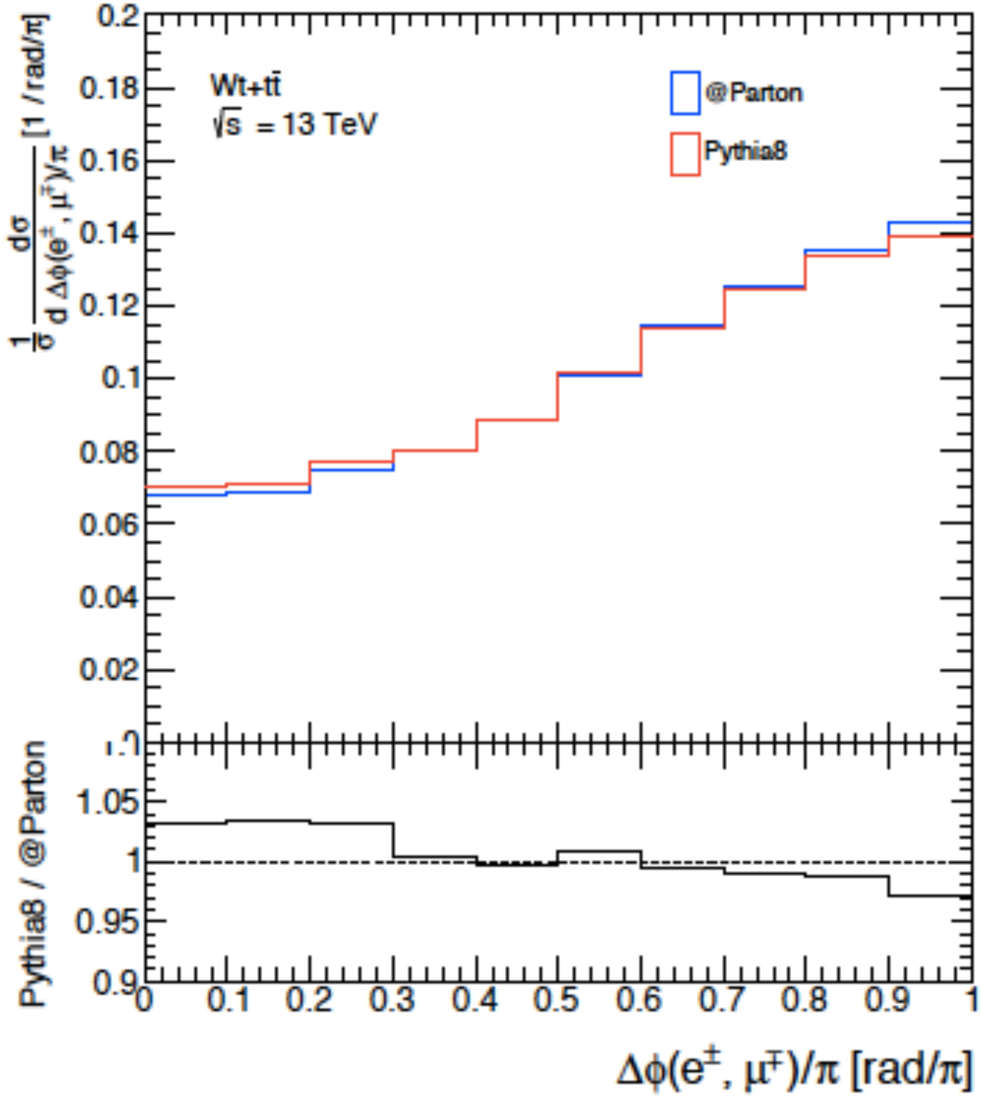

Impact of NNLO QCD in WW

The NNLO QCD corrections shift the m_{ll} spectrum towards larger values.

The discrepancy becomes larger in the region of interest with m_{ll}<100 GeV

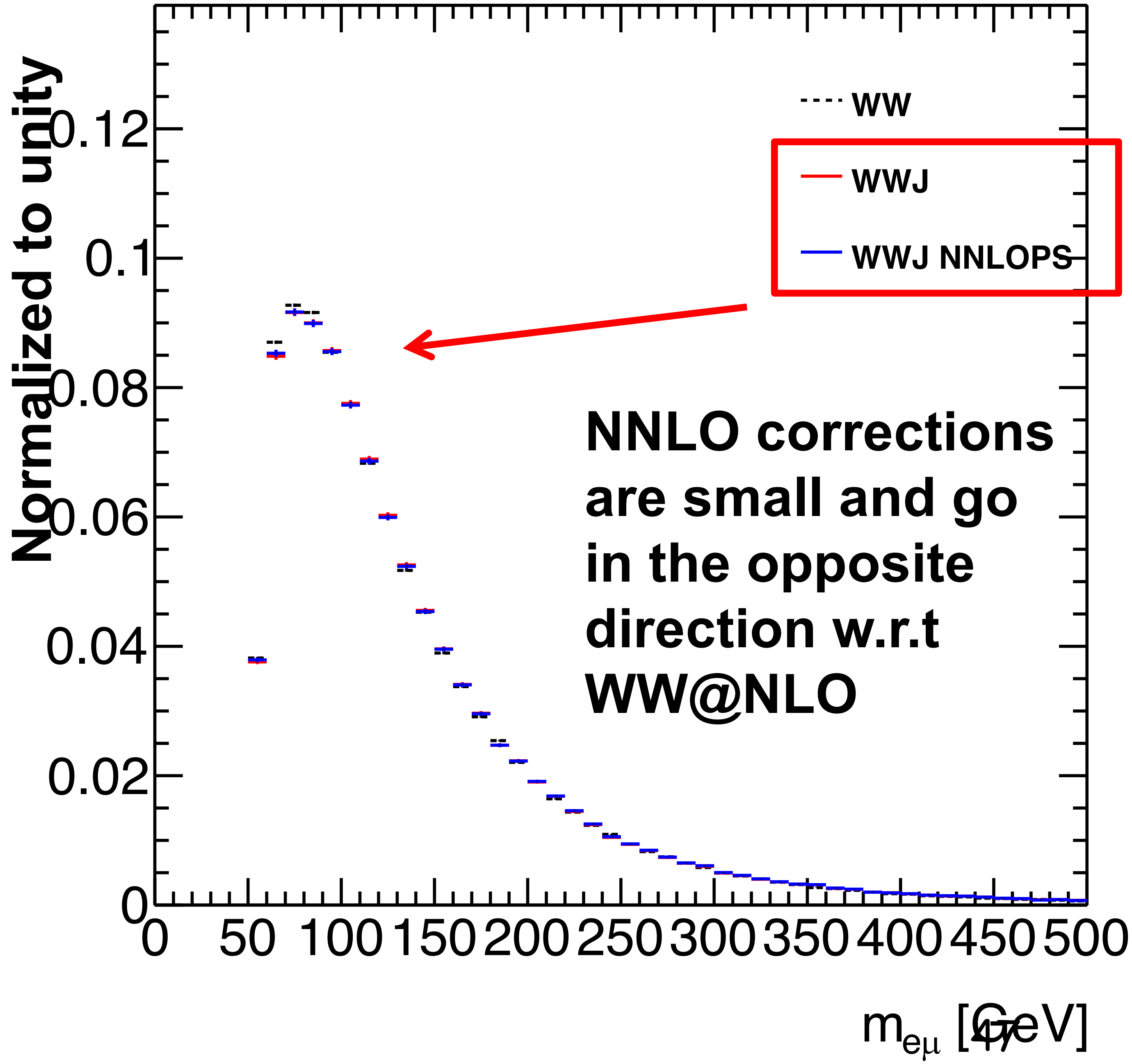

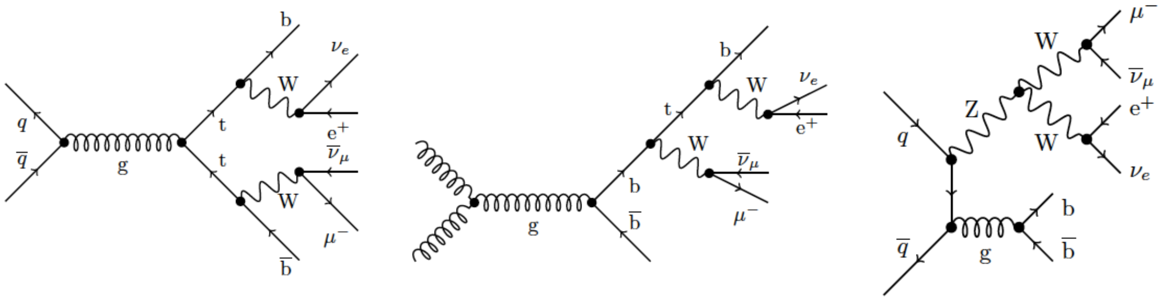

A.Denner, M.Pellen, arXiv:1607.05571

EW corrections are important at high p_T due to Sudakov logarithms.
Effect is less than 1% for m_{ll}<100 GeV, where discrepancies are seen.

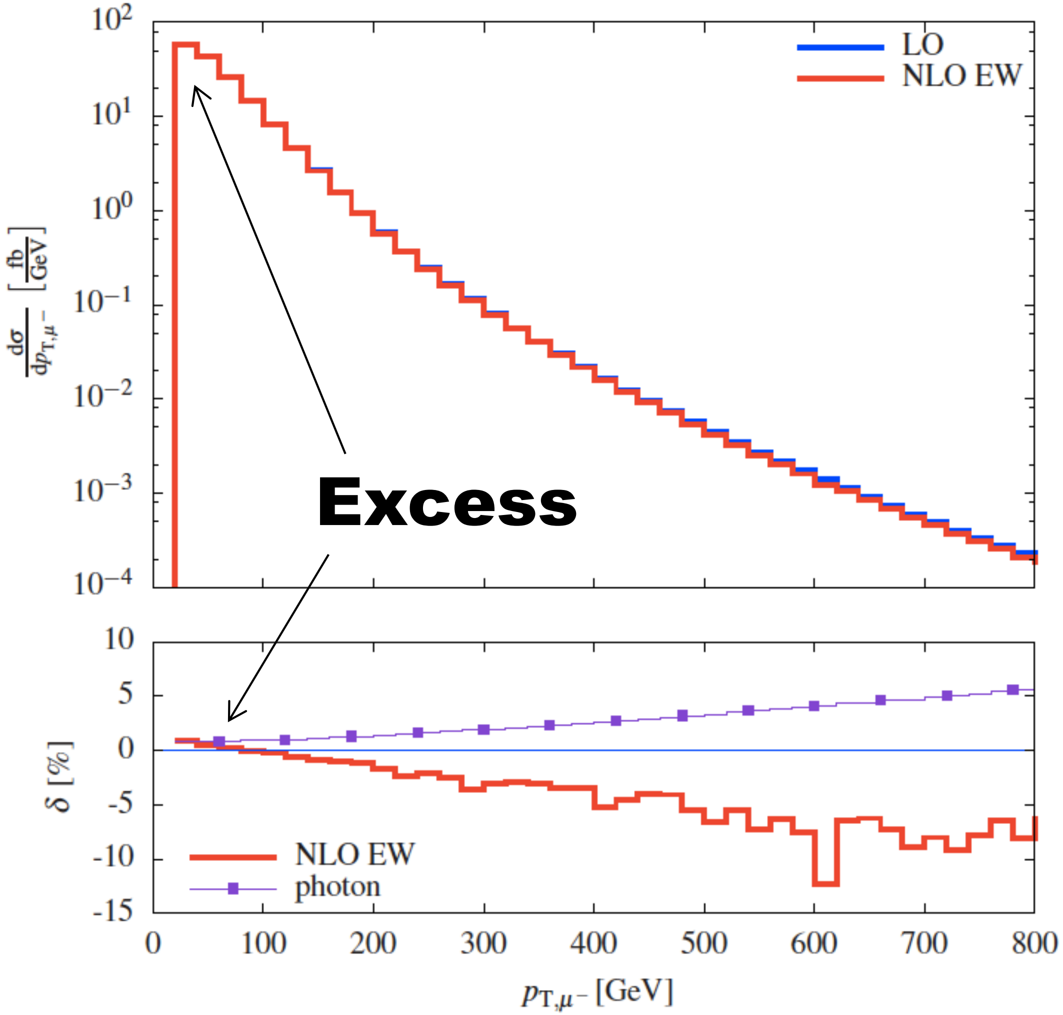

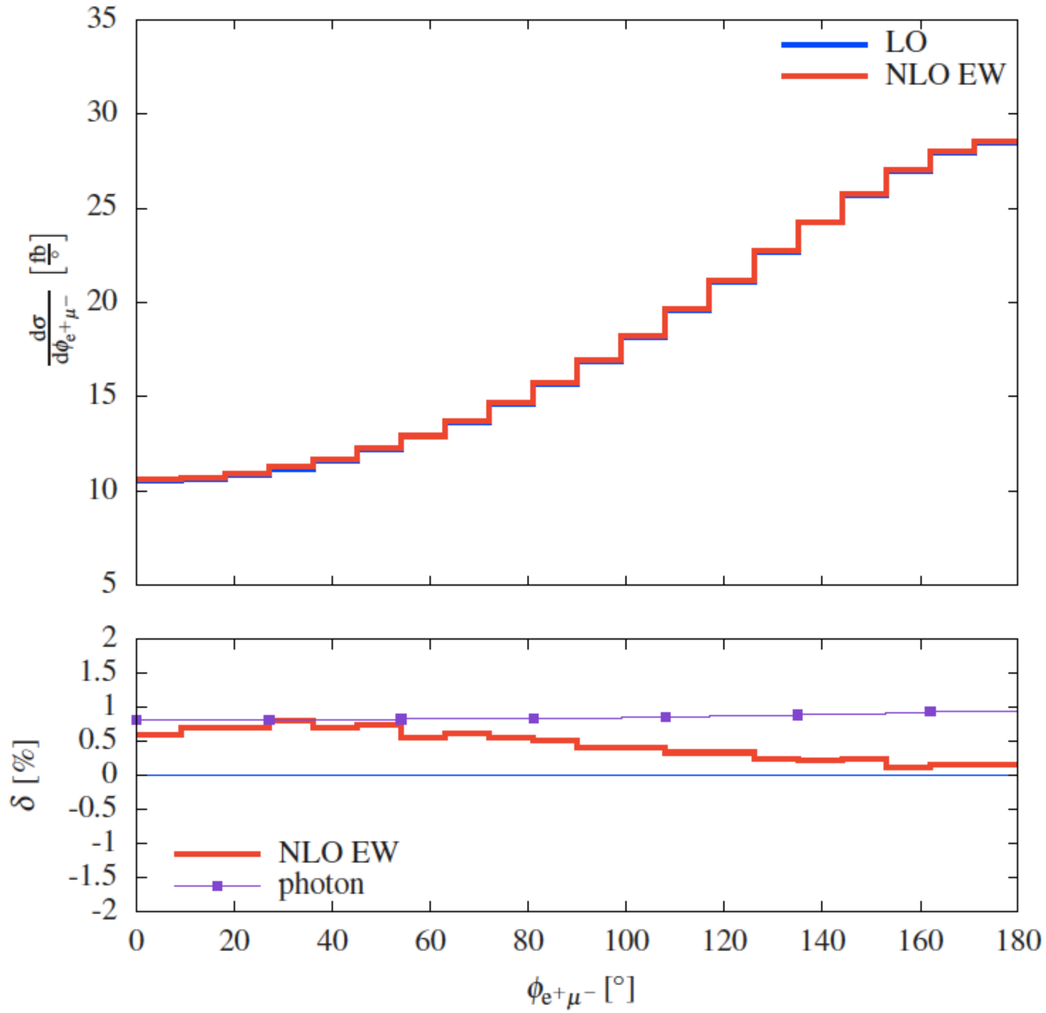

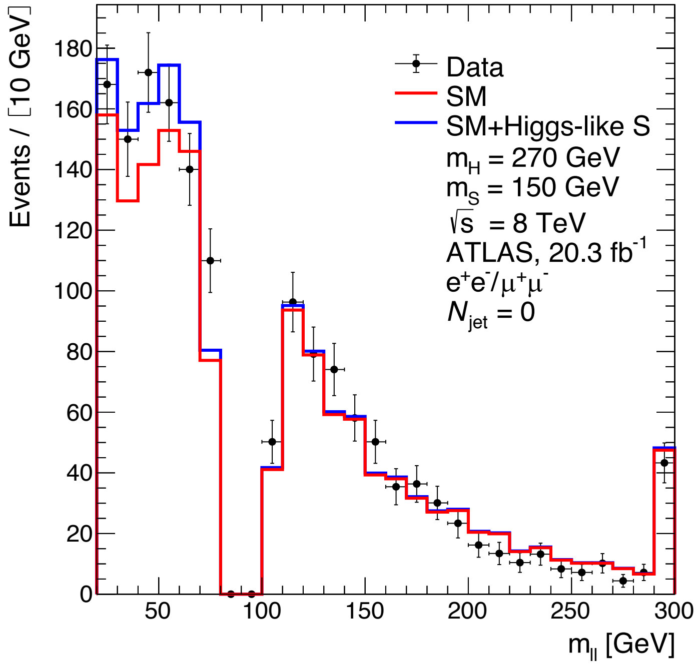

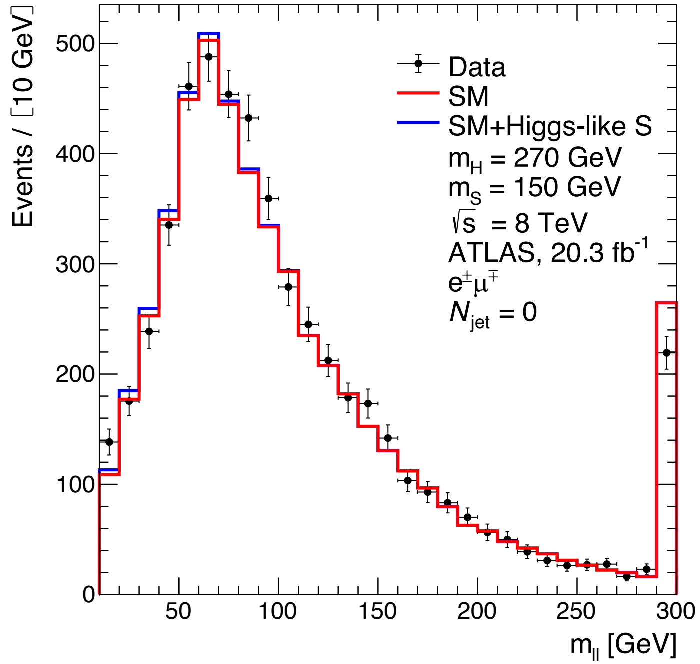

arXiv:1711.07874

Discrepancies in similar m_{ll} range also seems to appear in events **with a full jet (b-jet)** **veto with Run I data (in the context of the WW cross-section measurement. Potential impact on h→WW→ll analysis where the WW is normalized with relatively low m_{ll} (factors of 1.1-1.2, different from high masses).** **Issue does not seem tt-related**

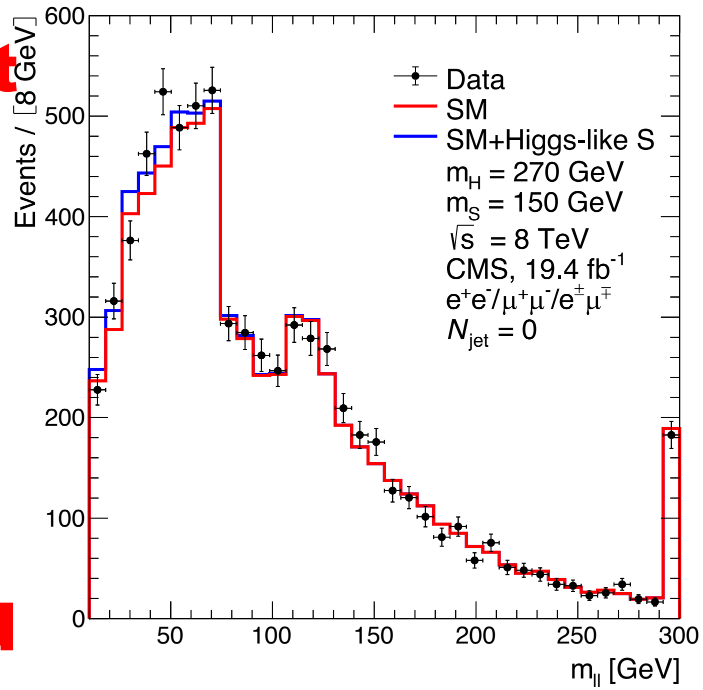

Results not included in combination as events are already included in top spin analysis

ATLAS-CONF-2018-004

Process	Matrix Element (Alternative)	PDF	PS (Alternative)	Precision σ
$t\bar{t}$	POWHEG-BOX v2 [38] SHERPA 2.2.1	NNPDF3.0NLO	PYTHIA 8 [39] (HERWIG 7)	NNLO+NNLL [40]
Wt	POWHEG-BOX v1 [41]	CT10 [35]	PYTHIA 6.428 [42]	NLO [41]

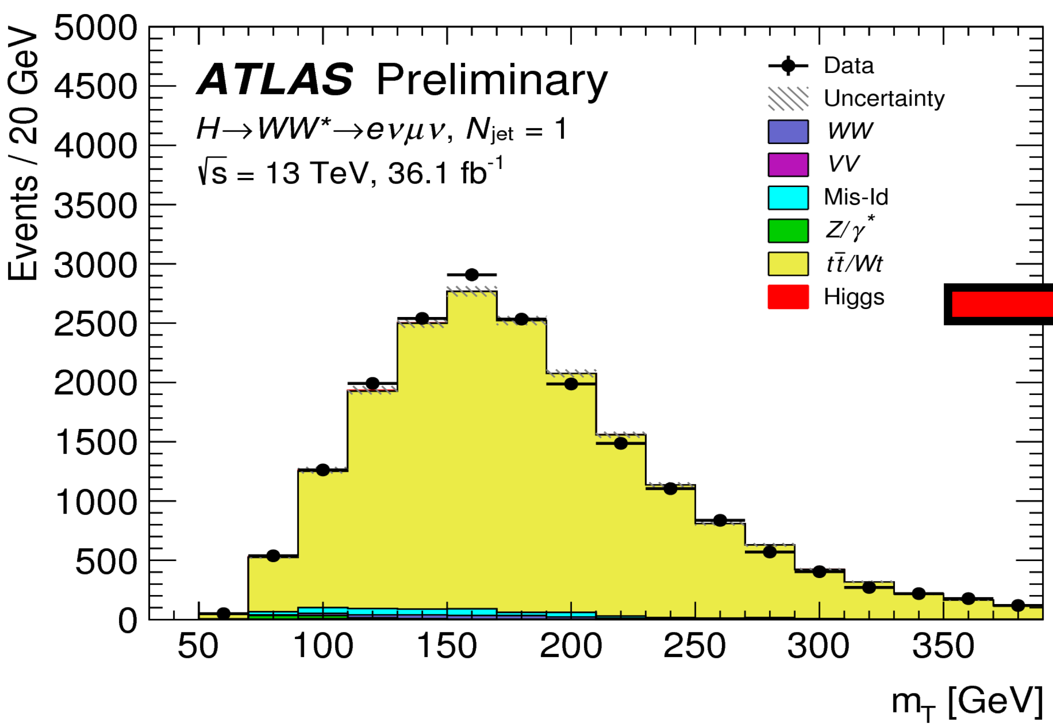

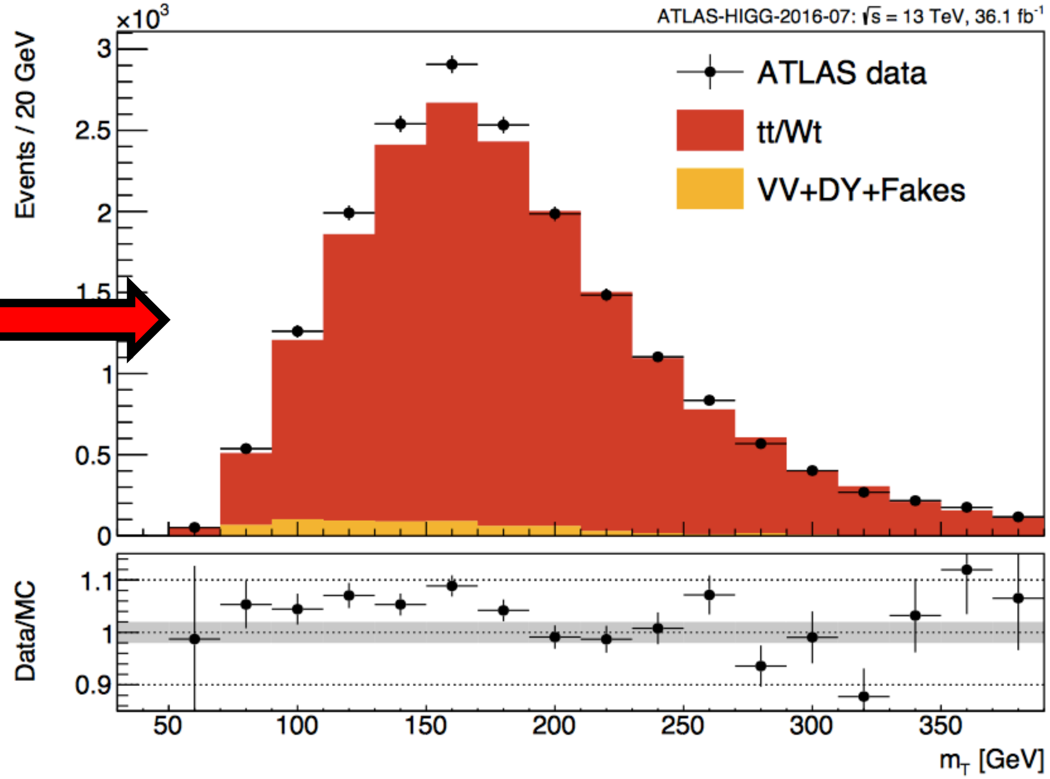

Top control sample with exactly two leptons, one b-jet and no more jets. Expect strong relative enhancement of Wt w.r.t. tt. MC studies in progress.

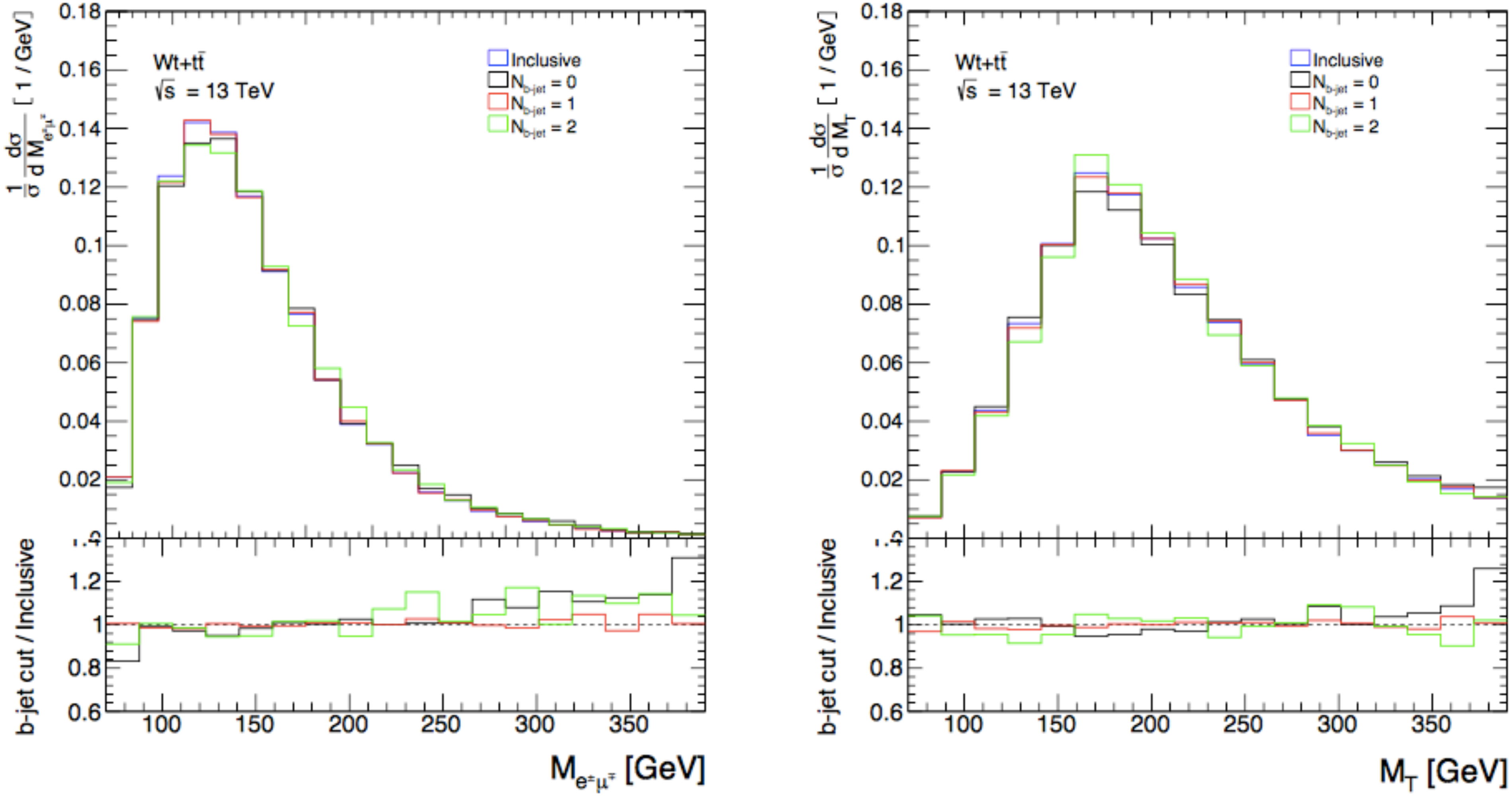

Di-lepton invariant mass depends little on the b-jet multiplicity

Figure 9: Leptonic distributions produced by $t\bar{t}$ and tW processes (see text) as a function of the b-tagged jet multiplicity. The di-lepton invariant mass (left) and the transverse mass of the di-lepton and missing transverse energy system are displayed. Distributions are normalised to unity. The insert shows the ratio of the distributions with exclusive b-tagged jet bins relative to that obtained inclusively.

CMS PAS TOP-17-014, https://cds.cern.ch/record/2621975/files/TOP-17-014-pas.pdf

None of the MCs studied is able to describe simultaneously the kinematics of top decay products. M_T of the dilepton and MET system is not shown

Table 3: The χ^2/ndof and p values quantifying the agreement between theoretical predictions and data for normalised, particle-level measurements are shown.

	POWHEG+PYTHIA8		POWHEG+HERWIG++		MG5_aMC@NLO+PYTHIA8	
	χ^2/ndof	p-val.	χ^2/ndof	p-val.	χ^2/ndof	p-val.
p_T^l (leading)	244/4	$< 10^{-3}$	5/4	0.332	75/4	$< 10^{-3}$
p_T^l (trailing)	163/4	$< 10^{-3}$	9/4	0.051	39/4	$< 10^{-3}$
$m_{l\bar{l}}$	143/7	$< 10^{-3}$	4/7	0.802	5/7	0.626
$\Delta\phi(l,\bar{l})$	35/9	$< 10^{-3}$	17/9	0.044	13/9	0.146
$\Delta\|\eta\|(l,\bar{l})$	7/9	0.635	5/9	0.798	7/9	0.626
N_{jets}	13/5	0.022	38/5	$< 10^{-3}$	90/5	$< 10^{-3}$
p_T^b (leading)	32/4	$< 10^{-3}$	75/4	$< 10^{-3}$	16/4	0.002
p_T^b (trailing)	28/4	$< 10^{-3}$	135/4	$< 10^{-3}$	19/4	$< 10^{-3}$
η_b (leading)	12/7	0.114	15/7	0.031	22/7	0.003
η_b (trailing)	16/7	0.024	16/7	0.021	12/7	0.105
$p_T^{b\bar{b}}$	25/4	$< 10^{-3}$	326/4	$< 10^{-3}$	38/4	$< 10^{-3}$
$m_{b\bar{b}}$	3/3	0.371	17/3	$< 10^{-3}$	1/3	0.751

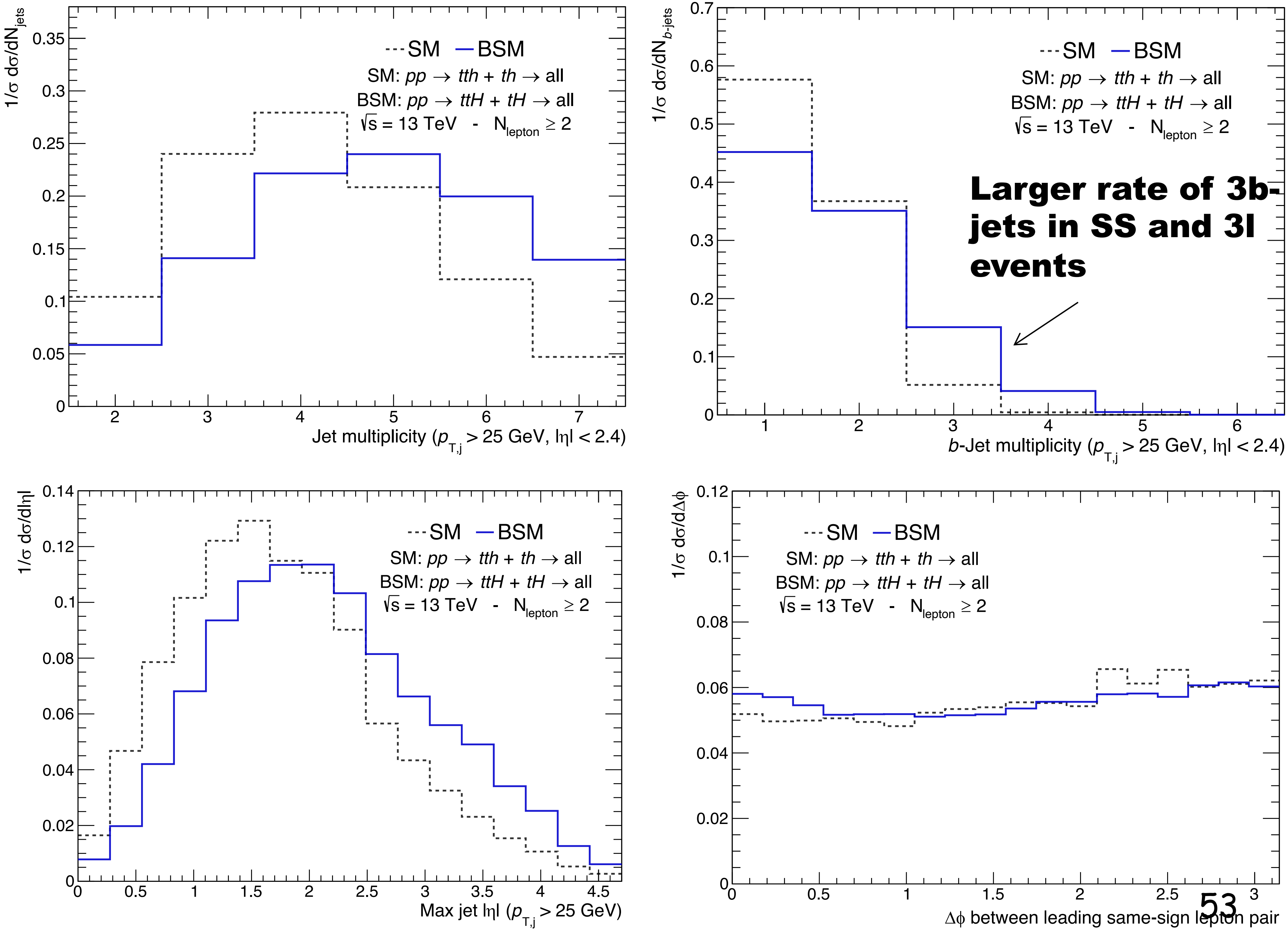

arXiv:1711.07874

SS leptons: CMS-PAS-HIG-17-005

- **CMS search for single top + Higgs production:**
  - **At least 2 SS leptons**
  - **At least 1 *b*-tagged jet**
- **The full analysis uses a BDT, so we compare to pre-selection plots**
- **Difficulty in estimating the probability of HF decay leptons to fake signal leptons**
  - **Not enough information in paper**
- **Fit results:**
  - $\beta_g^2 = 1.41 \pm 0.80$
  - **Weak measurement due to lack of statistics and large systematics**

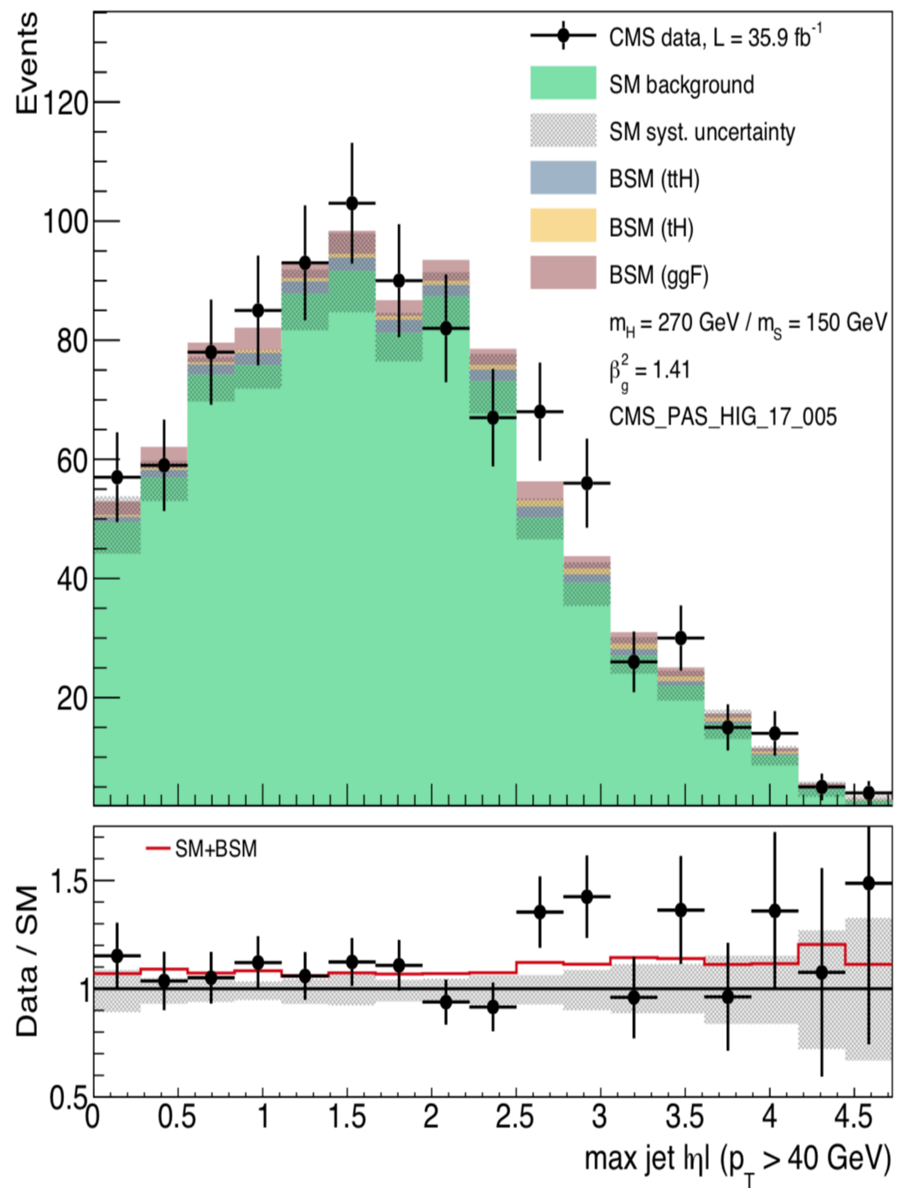

SS ll+b-jets: JHEP 10 (2015) 150

Definition			Name	
$e^{\pm}e^{\pm} + e^{\pm}\mu^{\pm} + \mu^{\pm}\mu^{\pm} + eee + ee\mu + e\mu\mu + \mu\mu\mu$, $N_j \geq 2$				
$400 < H_T < 700$ GeV	$N_b = 1$	$E_T^{miss} > 40$ GeV	SRVLQ0	
	$N_b = 2$		SRVLQ1	SR4t0
	$N_b \geq 3$		SRVLQ2	SR4t1
$H_T \geq 700$ GeV	$N_b = 1$	$40 < E_T^{miss} < 100$ GeV	SRVLQ3	
		$E_T^{miss} \geq 100$ GeV	SRVLQ4	
	$N_b = 2$	$40 < E_T^{miss} < 100$ GeV	SRVLQ5	SR4t2
		$E_T^{miss} \geq 100$ GeV	SRVLQ6	SR4t3
	$N_b \geq 3$	$E_T^{miss} > 40$ GeV	SRVLQ7	SR4t4
e^+e^+, $e^+\mu^+$, $\mu^+\mu^+$, $N_j \in [2, 4]$, $\Delta\phi_{\ell\ell} > 2.5$				
$H_T > 450$ GeV	$N_b \geq 1$	$E_T^{miss} > 40$ GeV	SRttee, SRtt$e\mu$, SRtt$\mu\mu$	

SS ll+b-jets: JHEP 10 (2015) 150

- **Final state search topology:**
  - 2 or 3 leptons (must be a same-sign pair)
  - At least 2 untagged jets
  - $E_T^{miss} > 40$ GeV, $H_T > 400$ GeV (binned into different signal regions)
- **Systematic uncertainty is large:**
  - In the fit, treated as a single normalisation uncertainty correlated over all SRs
- **Fit results:**
  - $\beta_g^2 = 6.51 \pm 2.99$
  - This is relatively high compared to other fit results

SR Key:
- 1 *b*-tagged jet: SRs 0, 3, 4
- 2 *b*-tagged jets: SRs 1, 5, 6
- ≥ 3 *b*-tagged jets: SRs 2, 7

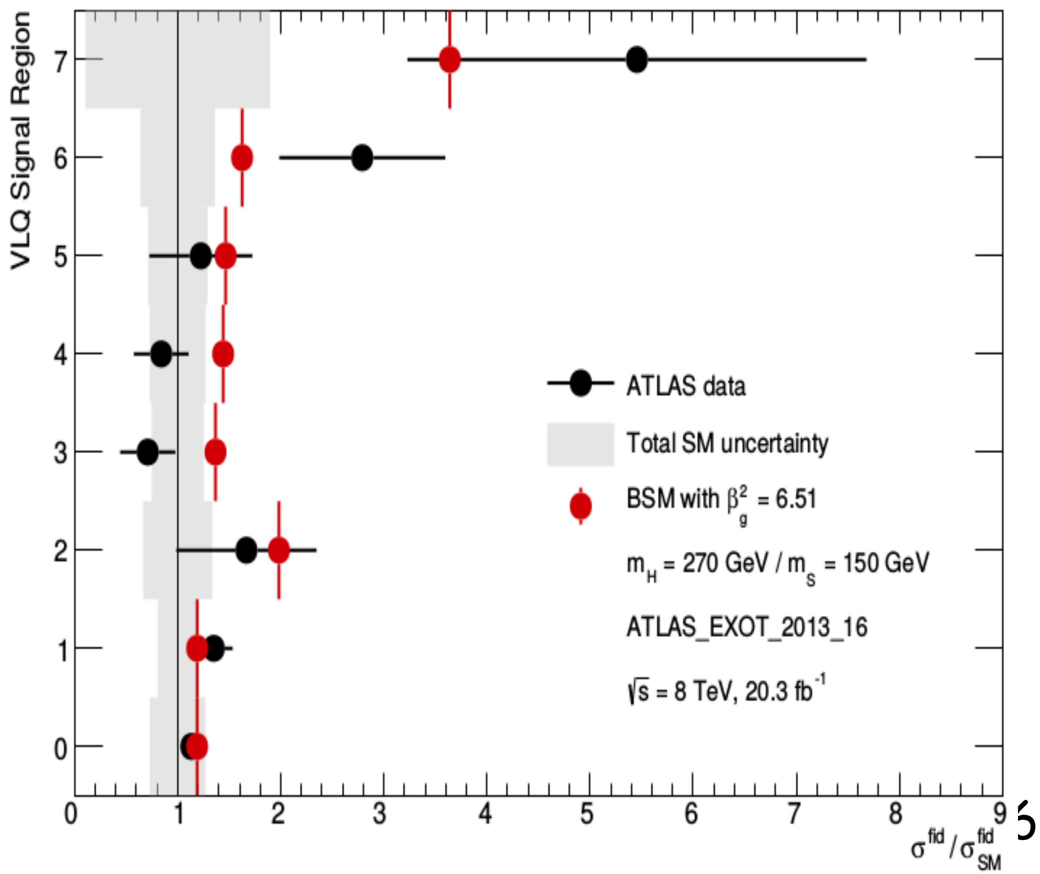

SS ll + b-jets: ATLAS-EXOT-2016-16

Region name	N_j	N_b	N_ℓ	Lepton charges	Kinematic criteria
VR1b2ℓ	≥ 1	1	2	++ or −−	$400 < H_T < 2400$ GeV or $E_T^{miss} < 40$ GeV
SR1b2ℓ	≥ 1	1	2	++ or −−	$H_T > 1000$ GeV and $E_T^{miss} > 180$ GeV
VR2b2ℓ	≥ 2	2	2	++ or −−	$H_T > 400$ GeV
SR2b2ℓ	≥ 2	2	2	++ or −−	$H_T > 1200$ GeV and $E_T^{miss} > 40$ GeV
VR3b2ℓ	≥ 3	≥ 3	2	++ or −−	$400 < H_T < 1400$ GeV or $E_T^{miss} < 40$ GeV
SR3b2ℓ_L	≥ 7	≥ 3	2	++ or −−	$500 < H_T < 1200$ GeV and $E_T^{miss} > 40$ GeV
SR3b2ℓ	≥ 3	≥ 3	2	++ or −−	$H_T > 1200$ GeV and $E_T^{miss} > 100$ GeV
VR1b3ℓ	≥ 1	1	3	any	$400 < H_T < 2000$ GeV or $E_T^{miss} < 40$ GeV
SR1b3ℓ	≥ 1	1	3	any	$H_T > 1000$ GeV and $E_T^{miss} > 140$ GeV
VR2b3ℓ	≥ 2	2	3	any	$400 < H_T < 2400$ GeV or $E_T^{miss} < 40$ GeV
SR2b3ℓ	≥ 2	2	3	any	$H_T > 1200$ GeV and $E_T^{miss} > 100$ GeV
VR3b3ℓ	≥ 3	≥ 3	3	any	$H_T > 400$ GeV
SR3b3ℓ_L	≥ 5	≥ 3	3	any	$500 < H_T < 1000$ GeV and $E_T^{miss} > 40$ GeV
SR3b3ℓ	≥ 3	≥ 3	3	any	$H_T > 1000$ GeV and $E_T^{miss} > 40$ GeV

SS ll+ b-jets: ATLAS-EXOT-2016-16

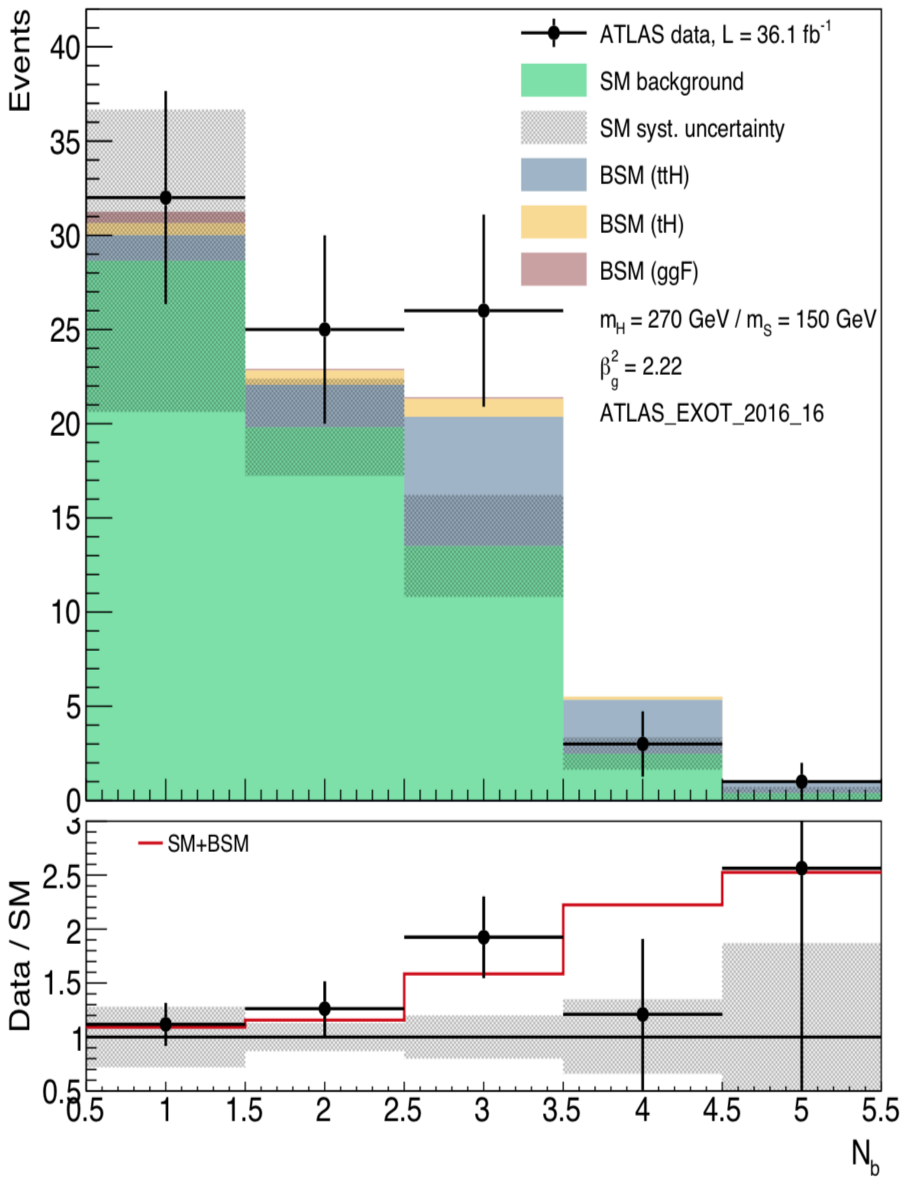

- **Run 2 version of SS + *b*-jet search:**
  - **At least 2 SS leptons**
  - **At least 1 *b*-tagged jet**
  - **Large E_T^{miss} and H_T**
- **Fit to inclusive SR distributions (auxiliary figures)**
- **Shows the strength of the model to fit the 3 *b*-jet excesses**
- **Fit results:**
  - $\beta_g^2 = 2.22 \pm 1.19$

Fit results: CMS-PAS-HIG-17-005

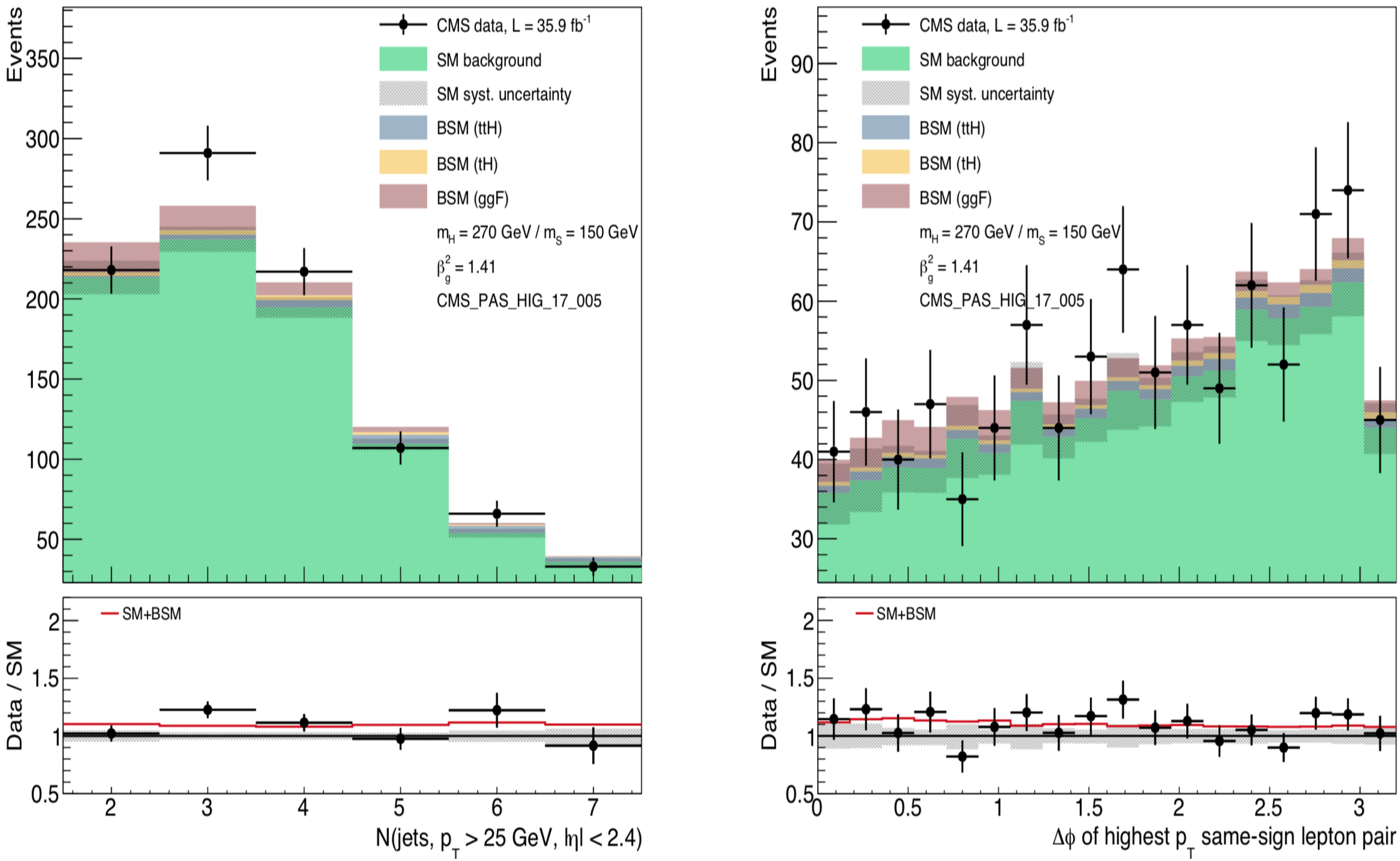

SS ll + b-jets: ATLAS-EXOT-2016-16

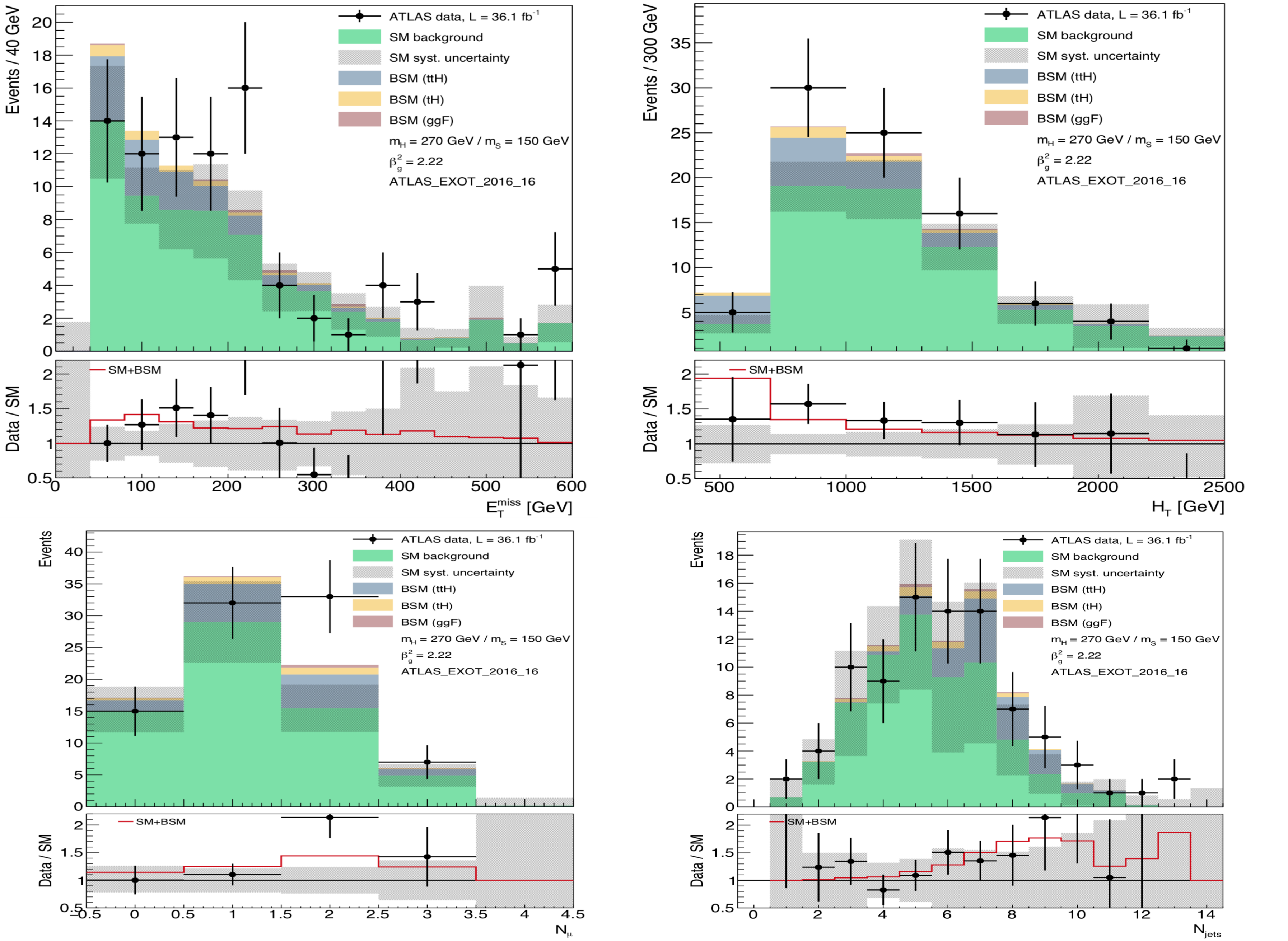

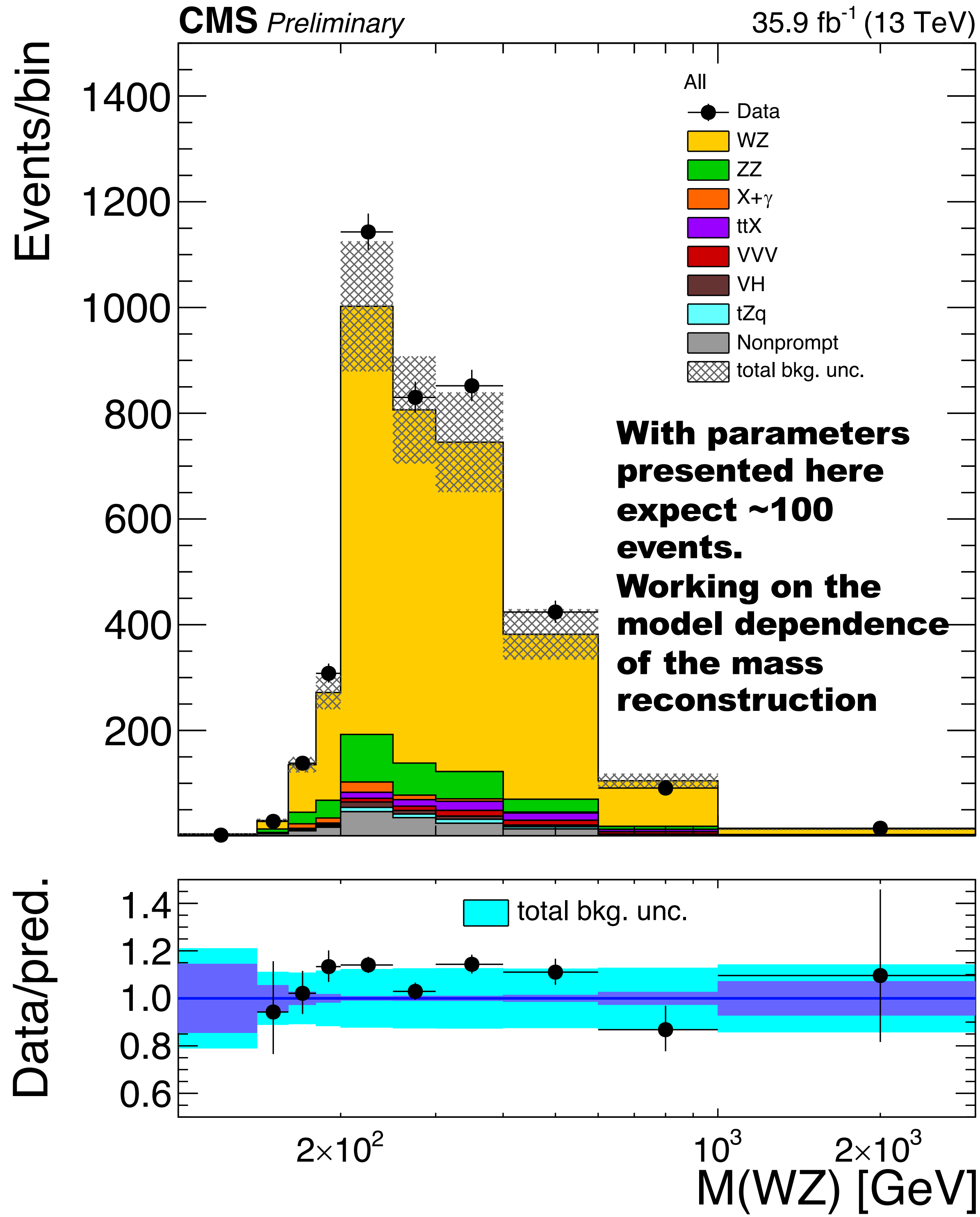

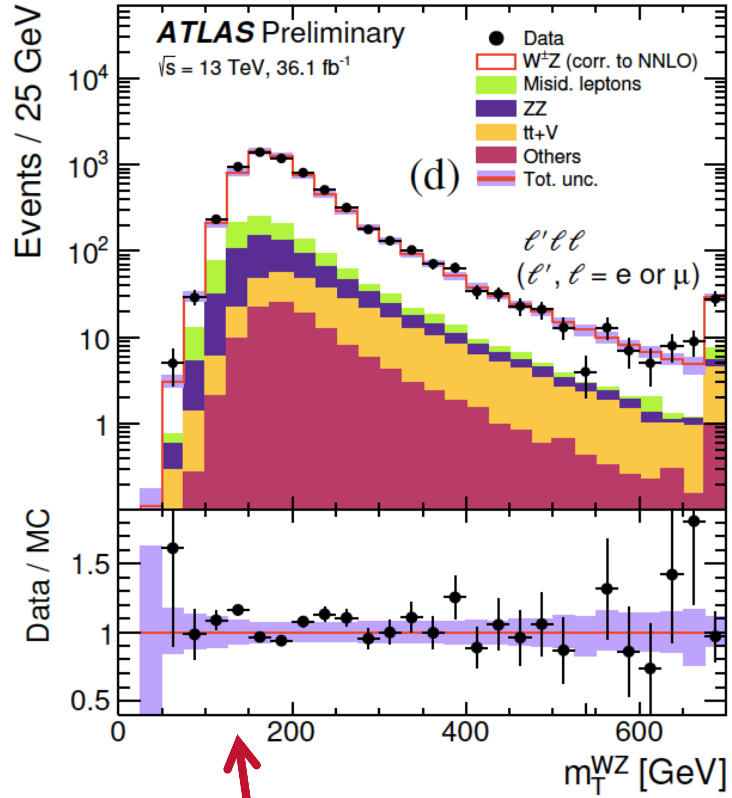

arXiv:1711.07874

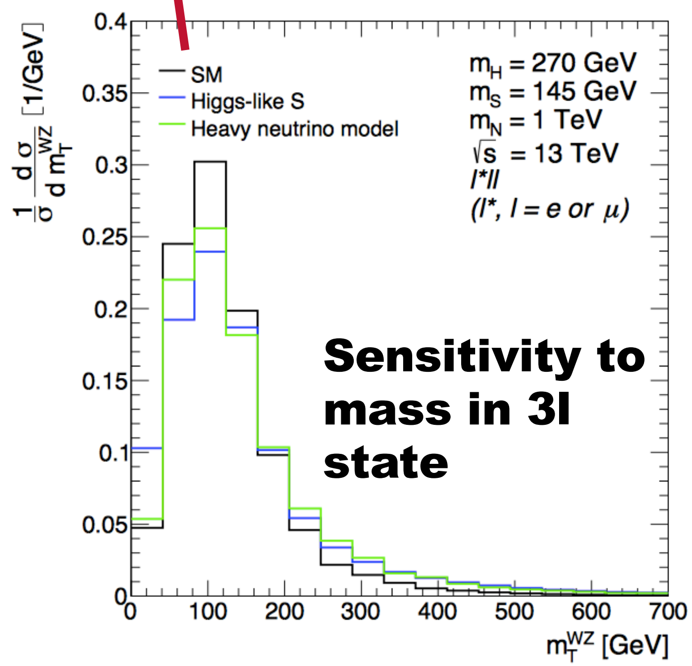

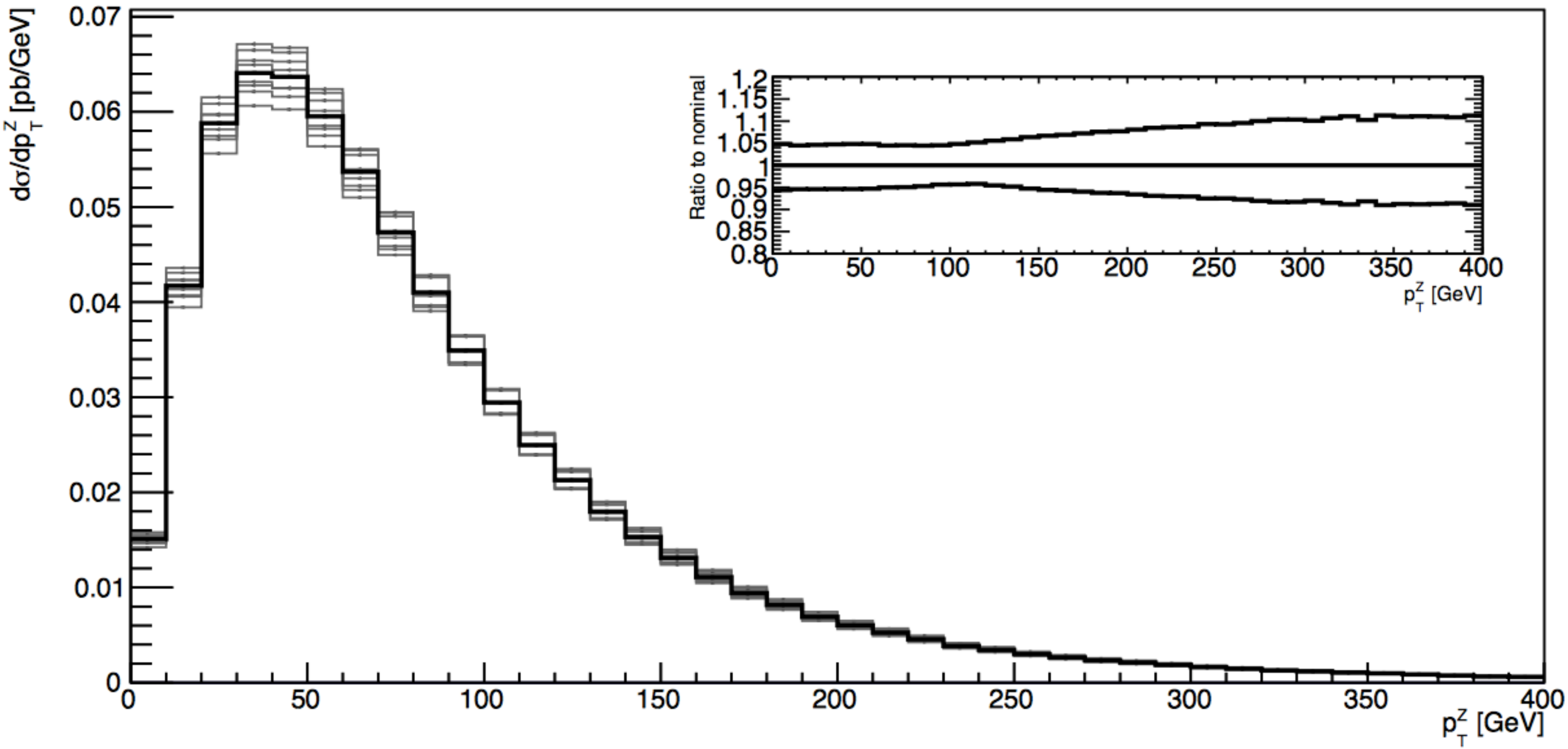

Figure 10: The effects of scale variations in the differential cross section of the SM WZ process as a function of the Z p_T. Here, `aMC@NLO` and `Pythia 8` were used to generate the events. The thick black line represents the spectrum at the nominal scale, and each grey line is a variation of the scale. The insert shows the maximum and minimum relative deviations for all scale variations.

The HistFactory method

K. Cranmer, G. Lewis, L. Moneta, A. Shibata, and W. Verkerke, *HistFactory: A tool for creating statistical models for use with RooFit and RooStats*, CERN-OPEN-2012-016.

- **Constructs a likelihood function from template histograms**
- **Allows for a simple implementation of systematic uncertainties that affect normalisation and/or shape**

$$\mathcal{P}(n_{cb}, a_p \,|\, \phi_p, \alpha_p, \gamma_b) = \prod_{c\in\text{channels}} \prod_{b\in\text{bins}} \text{Pois}(n_{cb}|\nu_{cb}) \cdot G(L_0|\lambda, \Delta_L) \cdot \prod_{p\in\mathbb{S}+\Gamma} f_p(a_p|\alpha_p)$$

In our case, each “channel” is a different measurement.

The Poisson probability for the “expected” and “observed” number of events per bin.

Functional form of luminosity and its variations (not necessary for us).

Functional form of systematic variation with nuisance parameter αp.

The fitting procedure

- **The RooStats workspace is made by HistFactory**
- **From the workspace, a profile likelihood ratio is calculated,**

$$\lambda\left(\beta_g^2\right) = \frac{L\left(\beta_g^2 \mid \hat{\hat{\theta}}\right)}{L\left(\hat{\beta}_g^2 \mid \hat{\theta}\right)}$$

(here θ denotes the nuisance parameters)

- **The best-fit value of β_g^2 is then calculated as the minimum of -2log(λ), with an error corresponding to a unit of deviation in this quantity from the best-fit point**
- **The significance is calculated as $\sqrt{-2 \log \lambda(0)}$, since $\beta_g^2 = 0$ corresponds to the SM-only hypothesis**